

USING ZEBRAFISH XENOTRANSPLANTATION TO STUDY
EWING'S SARCOMA AND INVESTIGATE THE ROLE OF
Y-BOX BINDING PROTEIN 1 IN METASTASIS

by

Chansey J. Veinotte

Submitted in partial fulfilment of the requirements
for the degree of Master of Science

at

Dalhousie University
Halifax, Nova Scotia
August 2012

© Copyright by Chansey J. Veinotte, 2012

DALHOUSIE UNIVERSITY

DEPARTMENT OF MICROBIOLOGY AND IMMUNOLOGY

The undersigned hereby certify that they have read and recommend to the Faculty of Graduate Studies for acceptance a thesis entitled “USING ZEBRAFISH XENOTRANSPLANTATION TO STUDY EWING’S SARCOMA AND INVESTIGATE THE ROLE OF Y-BOX BINDING PROTEIN 1 IN METASTASIS” by Chansey J. Veinotte in partial fulfilment of the requirements for the degree of Master of Science.

Dated: August 22, 2012

Supervisor: _____

Readers: _____

DALHOUSIE UNIVERSITY

DATE: August 22, 2012

AUTHOR: Chansey J. Veinotte

TITLE: USING ZEBRAFISH XENOTRANSPLANTATION TO STUDY
EWING'S SARCOMA AND INVESTIGATE THE ROLE OF Y-BOX
BINDING PROTEIN 1 IN METASTASIS

DEPARTMENT OR SCHOOL: Department of Microbiology and Immunology

DEGREE: MSc CONVOCATION: October YEAR: 2012

Permission is here with granted to Dalhousie University to circulate and to have copied for non-commercial purposes, at its discretion, the above title upon the request of individuals or institutions. I understand that my thesis will be electronically available to the public.

The author reserves other publication rights, and neither the thesis nor extensive extracts from it may be printed or otherwise reproduced without the author's written permission.

The author attests that permission has been obtained for the use of any copyrighted material appearing in the thesis (other than the brief excerpts requiring only proper acknowledgement in scholarly writing), and that all such use is clearly acknowledged.

Signature of Author

Table of Contents

List of Figures	vii
List of Tables	ix
Abstract	x
List of Abbreviations Used	xi
Acknowledgements	xiv
Chapter 1: Introduction	1
1.1 Ewing's Sarcoma	1
1.1.2 Ewing's Sarcoma Historical View	1
1.1.3 <i>EWS-FLII</i> Chromosomal Translocation	2
1.1.4 Ewing's Sarcoma Cell of Origin	3
1.1.5 Clinical Presentation & Diagnosis	4
1.1.6 Ewing's Sarcoma Treatment	5
1.2 Metastasis	9
1.2.1 Primary Tumour and the Factors that Promote Metastasis	10
1.2.2 The Metastatic Cascade	13
1.2.3 Epithelial to Mesenchymal Transition (EMT)	18
1.3 Y-box Binding Protein	19
1.3.1 Background	19
1.3.2 YB-1 and EMT	20
1.3.3 YB-1 and Cell Cycle Regulation	21
1.3.4 The Roles of YB-1 in Multidrug Resistance and Tumour Suppression	22

1.3.5 YB-1 and <i>EWS-FLII</i> in Ewing's sarcoma	25
1.4 Zebrafish as a Cancer Model	27
1.4.1 Zebrafish Background	27
1.4.2 Implications for Using Zebrafish to Study Cancer	29
1.5 Zebrafish Xenotransplantation	31
1.6 Rationale	38
Chapter 2: Methods	40
2.1 Zebrafish Husbandry & Housing	40
2.2 Cell Line	40
2.3 Cell Preparation and Labeling	41
2.4 Xenotransplantation	41
2.5 Live Cell Microscopy and Cell Proliferation Quantification	42
2.6 Cell Migration Assay	44
2.7 Statistical Analysis	46
Chapter 3: Results	48
3.1 TC32 ES Cell Lines Survive and Proliferate in Zebrafish Embryos.	48
3.2 TC32 ES Cells Exhibit Cellular Migration In vivo	49
3.3 The Zebrafish XT Model Enables the Direct Observation of Key Steps in Metastasis	50
3.4 TC32 YB-1 kd Cells Display Significantly Reduced Cellular Migration to the Tail	60
Chapter 4: Discussion	66
4.1 The Zebrafish XT Platform can be Used to Study ES	66
4.2 Zebrafish XT can be Used to Examine Specific Cancer Cell Behaviours	69

4.3 Using the Zebrafish XT Platform to Model Human Metastatic Events	71
4.4 Studying Early Metastatic Events (Neoangiogenesis) in the Zebrafish XT Platform	72
4.4.1 Targeting Angiogenesis in Ewing’s Sarcoma	74
4.5 YB-1 Promotes Migration and/or Metastasis of ES in the Zebrafish XT Model	75
4.6 YB-1 Upregulation may cause Increased Angiogenic Recruitment to Promote Metastasis	76
4.6.1 Determining the Downstream Factors of YB-1 that Promote ES Metastasis	78
4.7 Advantages and Limitations to the Zebrafish XT Platform	80
4.8 Conclusion	83
References	84
Appendix A: Relative Risk Estimates for TC32 ctrl Compared to Fixed TC32 ctrl cells	99
Appendix B: Relative Risk Estimates for TC32 ctrl Compared to TC32 YB-1 kd cells	100
Appendix C: Copyright Permission	101

List of Figures

Figure 1. An overview of the main primary tumour locations for Ewing's sarcoma (ES) and the regions associated with primary metastasis at the time of ES patient diagnosis.	7
Figure 2. Schematic of the key steps associated with successful cancer cell metastasis.	16
Figure 3. Diagram of the general structure of Y-box binding proteins.	24
Figure 4. <i>In vitro</i> migratory behaviour of both TC32 ctrl and TC32 YB-1 kd cells.	26
Figure 5. Wildtype (wt) and select mutant zebrafish lines.	32
Figure 6. Overview of XT cell labeling and injection procedures.	45
Figure 7. Anatomic regions of the zebrafish XT model and scoring scheme for cell migration assay.	47
Figure 8. TC32 ctrl cells can be injected, survive, proliferate and migrate in the zebrafish xenotransplantation platform.	53
Figure 9. <i>In vivo</i> cell proliferation rate of TC32 ctrl cells is delayed compared to proliferation rates <i>in vitro</i>.	54
Figure 10. TC32 ctrl cells displayed cell migration in 70% of total injected embryos at 120 hpi.	55
Figure 11. Live cell imaging of Fixed TC32 ctrl cell and TetraSpeck microsphere injected <i>casper</i> embryos revealed no observable cell migration.	56

Figure 12. No significant differences in proliferation are observed of either control experiment within 24 – 96 hpi.	57
Figure 13. TC32 ctrl cells display active cell migration to the tail regions at 120 hpi in 70% of embryos.	58
Figure 14. Using <i>tg(fli1a:eGFP) casper</i> embryos TC32 ctrl cells were observed interacting with host vasculature.	59
Figure 15. TC32 ctrl cells are capable of transitioning through the vasculature and extravasating into the tail tissue.	61
Figure 16. TC32 YB-1 kd cells displayed similar anterior cell behaviour, to that of ctrl cells, however do not exhibit frequent cell migration to the tail region.	63
Figure 17. <i>In vivo</i> cell proliferation rate of TC32 YB-1 cells is delayed compared to proliferation rates <i>in vitro</i>.	64
Figure 18. TC32 ctrl cells display increased of cell migration to the tail region in contrast to TC32 YB-1 kd and controls.	65

List of Tables

Table 1. Zebrafish cancer models (Modified from Stoletov and Klemke 2008)	28
Table 2. Human cancer cells that have been transplanted into 48 hours post fertilization zebrafish (Modified from Martina et al. 2012)	37

Abstract

The most unfavourable prognostic factor for Ewing's sarcoma (ES) is the presence of metastases. To date, a viable cancer model for ES metastasis has not been developed. Models for ES are crucial to uncovering the key molecular mechanisms that are responsible for metastasis. Therefore, we developed a zebrafish xenotransplantation model to better visualize and manipulate ES behaviour *in vivo*. Human ES TC32 cells were fluorescently labeled with Cm-DiI, and microinjected into the yolk sac of two-day-old *casper* embryos. TC32 cells successfully engrafted, survived, proliferated and migrated over 144 hours post-injection (hpi). Y-box binding protein 1 (YB-1) is highly expressed in a variety of cancers and plays a key role in promoting breast cancer metastasis. In contrast to TC32 cells with regular levels of YB-1, xenografted YB-1 knockdown TC32 cells showed significantly reduced migration. These studies highlight the utility of the zebrafish xenograft model to elucidate the mechanisms underlying the metastatic behavior of ES and position this system as an *in vivo* tool for drug discovery to identify novel anti-proliferative and anti-metastatic agents to improve outcome in this disease.

List of Abbreviations Used

AB	‘wild-type’ zebrafish strain
AKT	Protein Kinase B
ATRA	all-trans retinoic acid
Bf	Brightfield
CaCl ₂	Calcium Chloride
CD__	Cluster of differentiation (number)
CD99	Cluster of differentiation 99
CDKs	Cyclin-dependent kinases
Cm-Dil	chloromethylbenzamido
CNS	central nervous system
CSCs	Cancer stem cells
CSD	Cold shock domain
CT	Computed tomography
Ctrl	Control
DFS	Disease free survival
DNA	Deoxyribonucleic acid
dpf	Days post fertilization
ECM	Extracellular matrix
EDTA	Ethylenediaminetetraacetic acid
eGFP	Enhanced green fluorescent protein
EMT	Epithelial to mesenchymal transition
ERG	Ets related gene
ES	Ewing’s sarcoma, thesis specific abbreviation
ESFTs	Ewing’s sarcoma family of tumours
Ets	Erythroblast transformation sequence

EWS	Ewing's sarcoma gene, in reference to translocations
FBS	Fetal bovine serum
FGF	Fibroblast growth factor
Fl	Fluorescent
Fli1	Friend leukemia integration 1
Flk1	Fetal liver kinase 1
gata1a	GATA-binding factor 1a
g	Gravity
GFP	Green fluorescent protein
Gy	Gray, unit of absorbed dose of irradiation
h	Hours
hpf	Hours post fertilization
hpi	Hours post injection
kd	Knockdown
kDa	Kilodalton
μg	Microgram
mg	Milligram
μl	Microliter
ml	Milliliter
min	Minutes
MMPs	Matrix-metalloproteinases
mpeg1	Macrophage expressed gene 1
mpo	Myeloperoxidase
MRI	Magnetic resonance imaging
MSCs	Mesenchymal stem cells
PBS	Phosphate buffered saline

PNETs	Peripheral neuroectodermal tumours
rpm	Revolutions per minute
RPMI	Roswell Park Memorial Institute
shRNA	Short hairpin ribonucleic acid
siRNA	Small interfering ribonucleic acid
S phase	DNA synthesis phase of cell cycle
T-ALL	T-cell acute lymphoblastic leukemia
tg	Transgenic
UV	Ultraviolet
VAC	Vincristine-actinomycin-cyclophosphamide
VACD	Vincristine-actinomycin-cyclophosphamide-doxorubicin
VEGF	Vascular endothelial growth factor
wpf	Weeks post fertilization
WT	Wildtype
X	times
XT	Xenotransplantation
YB-1	Y-box binding protein 1

Acknowledgements

I would like to first and foremost thank my supervisor Dr. Jason Berman, whose guidance, support, and mentorship has assisted me immensely in the completion of this thesis. I would also like to thank Dale Corkery for all of his mentorship during my research project.

I would like to thank the members of my committee Dr. Graham Dellaire, Dr. Jean Marshall, Dr. Mark Bernstein and Dr. Poul Sorensen for the support and guidance throughout my research project. Special thanks to Dr. Krista Ritchie for her assistance with the SPSS analysis of my data.

I would also like to thank all the members of the Berman and Dellaire laboratories for their assistance and friendship throughout this project. Last but not least, I would like to thank all of my family and friends for their support throughout my research.

Chapter 1: Introduction

1.1 Ewing's Sarcoma

The Ewing's sarcoma family of tumours (ESFTs) is a group of rare aggressive childhood cancers including classic Ewing's sarcoma, Askin tumour and peripheral neuroectodermal tumour or primitive neuroectodermal tumour (Balamuth and R. B. Womer 2010; Ludwig 2008; Puchalski 2010). Ewing's sarcoma (ES) is the second most common bone cancer seen in children. Advances in treatment have made significant improvements in the 5 year disease free survival (DFS) of children with localized ES disease to approximately 75%, while children diagnosed with metastatic disease fair much worse with an estimate 20-25% 5 year DFS. Many researchers have focused their efforts on determining what mechanisms cause metastasis and how these events can be stopped to save the lives of many people diagnosed with cancer.

1.1.2 Ewing's Sarcoma Historical View

First characterized and published, in 1921 by American pathologist James Ewing, ES was described as a group of small round cells with high nuclear to cytoplasm ratios, that develop into densely packed cell sheets. He described the disease as an "endothelial myeloma" of the bone tissue (Peltier 1984)(Ewing, 1921). Though morphologically similar to the other ESFTs, Ewing's sarcoma is the second most common form of bone cancer observed in children and young adults after osteosarcoma. Approximately 250 people are diagnosed with ES in North America every year, with an average of three out of every one million people developing ES. ES is a relatively rare form of cancer observed most

frequently in children ages 10-15 years old, with a slight male predominance (1.3:1). Of the worldwide population, there is a notable discordance between races with more whites than any other group being diagnosed with ES. To date there has been no clear explanation for these observations (Hense et al. 1999). ES is ascribed to be a spontaneous cancer caused by specific genetic translocations, rather than a result of specific environment conditions or genetic predisposition.

1.1.3 *EWS-FLI1* Chromosomal Translocation

A chromosomal translocation involves the mechanical breaking and reconnection between different regions of two chromosomes, which results in the genetic content housed on those chromosomes to become altered. Generally, ES is characterized by the presence of a chromosomal translocation between the *EWS* gene (Ewing's sarcoma breakpoint region 1 – EWSR1) on chromosome 22 and a member of *Ets* (erythroblast transformation sequence) family of transcription factors. A translocation between chromosome 11 and 22 $t(11;22)(q24;q12)$ is observed in about 85% of all patients diagnosed with ES (Bernstein et al. 2006; Ludwig 2008). This chromosomal rearrangement results in the fusion gene product *EWS-FLI1*. The *EWS* gene, on chromosome 22, is an RNA-binding protein of unclear function in humans however recent studies in zebrafish involving the orthologs (*ewsr1a* and *ewsa1b*), demonstrates that *EWS* may act on mitotic integrity and proneural cell survival of the CNS (Azuma et al. 2007). *FLI-1*, on chromosome 11, is a transcription factor belonging to the *Ets* family, known to be important for embryological development, hematopoiesis, angiogenesis and cell growth and differentiation in humans (Plougastel et al. 1993). *FLI-1* is

expressed in the developing vasculature of humans, mice and zebrafish (Brown et al. 2000; Hart et al. 2000).

It has been shown that neither overexpression of *EWS* or *FLI-1* alone is capable of inducing ES (Ludwig 2008). It is suggested that their fusion, found in the majority of ES, promotes a cooperative action including enhanced transcriptional activity, which ultimately results in malignant transformation (Bernstein et al. 2006; Ludwig 2008; Balamuth and Worner 2010). Cases of ES that lack the *EWS-FLII* fusion usually have *EWS* paired with another member of the *Ets* family such as the transcription factor *ERG* (ETS-related gene) (Sorensen et al. 1994; Shing et al. 2003). The fusion of the *EWS* gene to different members of the *Ets* family such as *FLI-1* or *ERG* results in developmentally and morphologically similar ES phenotypes. Further comparison between these *Ets* genes revealed comparable fusion points to *EWS* and very similar gene structures, which may explain why their fusion to *EWS* results in similar ES disease (Ginsberg et al. 1999). These same chromosomal translocations have been identified in both localized and metastatic ES, however, they are not prognostic (Le Deley et al. 2010; van Doorninck et al. 2010).

1.1.4 Ewing's Sarcoma Cell of Origin

While there is some speculation on the specific cell(s) of origin for ES it is generally becoming more and more accepted that mesenchymal progenitor/stem cells (MSCs) may be the most likely candidate population of origin. It has been shown that MSCs can be induced into an ES state by the overexpression of *EWS-FLII* (Nicolò Riggi and Stamenkovic 2007; Nicolò Riggi et al. 2008). These cells, when introduced into a xenograft mouse, were unable to form tumours but did display significantly increased levels of ES specific surface markers including

CD99 (discussed later) and standard ES morphology. Cooperatively, it has been shown that when ES cells *in vitro* are subjected to a stable shRNA knockdown of *EWS-FLII*, they revert back to a phenotype characteristic of human MSCs, with specific markers such as CD44 and CD73, and notably trilineage differentiation plasticity capabilities, classically displayed by MSCs (Nicolo Riggi, Suva, and Stamenkovic 2009; Tirode et al. 2007). Although MSCs are gaining significance, as the precursor cell of choice for ES, further studies are needed to confirm this hypothesis.

1.1.5 Clinical Presentation & Diagnosis

Patients with ES often present with variable degrees of pain associated with a particular region where a palpable mass will likely later follow (Bernstein et al. 2006; Heare, Hensley, and Dell’Orfano 2009). ES lesions may occur in any bone but are frequently located in the diaphysis (mid region) of long bones, compared to the metaphyseal regions (wide bone regions above and below the diaphysis), which are associated with osteosarcoma (Heare, Hensley, and Dell’Orfano 2009). ES is frequently associated with a soft tissue component and in some cases may, in fact, arise from soft tissues without involving bone. The duration of these initial symptoms, prior to a definitive diagnosis, can average between three to nine months. To confirm the diagnosis several forms of imaging may be used including plain radiography, magnetic resonance imaging (MRI), or computed tomography (CT), along with a biopsy of the tissue or mass in question. A plain radiograph may reveal ES lesions with an onion-skin pattern, while in other cases, ES lesions may appear as “hair on end”, calcified spicules that arise perpendicular to bone surface, in periosteal bone formation. Biopsied tissue can be analyzed for specific pathologic markers for ES. One such

marker is CD99, which is highly expressed in 95-100% of ESFTs (I. M. Ambros, P. F. Ambros, and Strehl 1886). CD99 is a 32 kDa cell surface glycoprotein, encoded by the MIC2 gene that is used by pathologists to confirm ESFTs. CD99 is also expressed in other cell types, which limits its use for a sole diagnostic tool/marker (Zhang et al. 2000). Neuronal markers such as S-100 protein, neuron-specific enolase and synaptophysin are used to further distinguish between different cell types and specific ESFTs, during diagnosis (Schmidt et al., 1991). Tumours that lack neuronal markers are likely ES while those with two or more of the markers are termed peripheral neuroectodermal tumours (PNETs). Following confirmation, patients typically undergo staging studies, including bone marrow aspiration, biopsy, and whole body imaging to determine disease/tumour burden and whether or not the disease has spread or metastasized.

The most common sites of localized ES include, but are not limited to, the chest wall, the pelvis, the femur and the tibia. The lungs, other bones and the bone marrow are often the most frequent sites for metastasis (Figure 1).

1.1.6 Ewing's Sarcoma Treatment

Prior to the development of advanced chemotherapeutics, the 5 year DFS for localized ES was less than 10%. With the development of modern multimodal therapeutic regimens including chemotherapy, surgery and radiotherapy, ES patients, with local disease, have a significantly improved 5 year DFS of approximately 75% (Paulussen et al., 2001).

Chemotherapy for ES began in the 1960s, initially with single drug treatments using cyclophosphamide, doxorubicin, vincristine, dactinomycin and carmustine. These treatment options were followed by the development of multimodal adjuvant chemotherapy trials

using vincristine-actinomycin-cyclophosphamide (VAC) or VAC plus doxorubicin (VACD). VAC together with doxorubicin was shown by the Intergroup Ewing's Sarcoma Study, conducted 1972-1978, to be more effective in combination compared to VAC alone. Local control and DFS could be improved with the newly used VACD, however, with increasing doses of doxorubicin, greater cardiac toxicities were observed (Nesbit et al., 1990; Burgert et al., 1990). Further studies, such as those conducted through the Children's Cancer Group-Pediatric Oncology Group, showed that ifosfamide and/or etoposide, in addition to VACD, resulted in even more effective outcomes of 70% 5 year DFS for patients with localized disease (Craft et al., 1998; Grier et al., 2003).

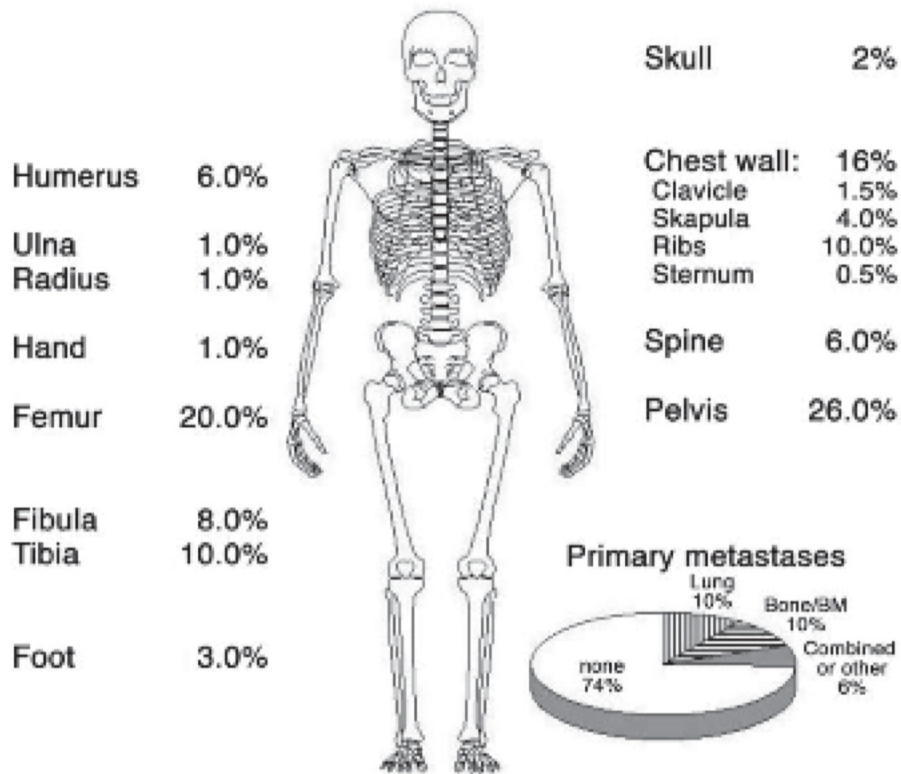


Figure 1. An overview of the main primary tumour locations for Ewing's sarcoma (ES) and the regions associated with primary metastasis at the time of ES patient diagnosis. The most common sites of ES are the pelvis, femur, chest wall and tibia. Primary metastases discovered at diagnosis are often found in the lungs or in other bones/bone marrow. Figure reproduced from Bernstein et al., 2006 with permission (Appendix D).

Current treatment regimens vary depending on the condition of the ES patient and the progression of the cancer. Vincristine, cyclophosphamide, doxorubicin, ifosfamide and etoposide are consistently partnered chemo-agents that make up the five-drug regimen standard therapy used as a primary ES treatment in most of North America.

Chemotherapy, though effective at treating many cases of ES, is associated with a number of harmful toxicities. Chemotherapy causes patients to become severely immunocompromised and unable to fight off various infections due to periods of neutropenia (Crawford, Dale and Lyman 2003). Some forms of cancer may become resistant to some of the drugs used, making them an ineffective treatment option (J. F. Kuttesch 1996). During treatment patients may experience nausea, vomiting, anemia and low platelet counts, however there are different drugs that are used concurrently to mitigate some of these side effects. In addition, a significant psychological burden caused by chemotherapy is alopecia (loss of hair), which frequently causes significant patient angst and can be emotionally very traumatic. However hair generally grows back following the completion of treatment. The long-term effects of chemotherapy include cardiac abnormalities (myocardial ischemia and severe arrhythmias), secondary malignancies and gonadal dysfunction (infertility) (Monsuez et al. 2010; Fleischer et al. 2011).

Though ES are generally radiation sensitive (Ewing, 1939), the proportion of patients who receive radiation alone is declining due to advances in other treatment methods with less harmful long-term effects. Radiation may be used cooperatively with surgical resection and chemotherapy to treat ES. When administered for local disease, 45-50 Gray (Gy) of radiation are used to treat ES over multiple week intervals. Radiotherapy is also associated

with several side effects including chronic swelling, joint stiffness and secondary cancers later in life due to the damage that it may cause to healthy cells in the body (B. J. F. Kuttesch et al. 2012). ES is an aggressive cancer that can require close to a year to complete treatment. Fourteen to seventeen cycles of chemotherapy with alternating drug regimens are often administered along with surgical resection if possible. Ultimately, a patient who does not respond to current treatment options may be a candidate for therapeutic alternatives such as novel drugs currently in Phases I or II of clinical trials.

Though tremendous progress has been made in the refinement of therapeutic management of localized ES the treatment of metastatic ES has not seen the same advances. The use of localized disease regimens, even with greatly increased chemotherapy drug concentrations and different combinations, has had no effect on metastatic ES (Bernstein et al. 2006; Ludwig 2008; Balamuth and Worner 2010). Approximately 25% of all ES patients will have metastatic disease at the time of diagnosis. Patients with metastases outside the lungs or with significant burden elsewhere, at diagnosis, seldom survive (Bernstein et al. 2006; Pauluseen et al. 2009). These results have led to many studies interested in further increasing the extent of chemotherapy issued to these patients including the addition of total body irradiation. These attempts have subsequently lead to minute improvements, which to date, have still inadequately addressed the treatment of metastatic ES (Granowetter et al. 2009; Windsor et al. 2009).

1.2 Metastasis

Metastasis is one of the most important aspects of cancer progression as it accounts for 90% of all cancer deaths (Mehlen and Puisieux 2006; D. X. Nguyen, Bos, and Massagué

2009). During the development of all cancers there is the chance that some cancer cells, from an original primary tumour site or location, will gain the potential to migrate or move to other sites within the human body (metastasis). This migration enables further colonization by cancer cells and allows their access to new resources that facilitates tumour cell growth into secondary metastases or tumours. This increased tumour burden often leads to the death of many people affected by cancer.

The exact mechanisms that influence and govern the metastatic capabilities of ES remain unclear. Since metastasis is the most important prognostic factor for therapeutic outcome in ES, it is crucial to investigate how these cells are able to spread so efficiently so that new therapeutic strategies can be developed, and those currently used revised, to improve patient outcome.

1.2.1 Primary Tumour and the Factors that Promote Metastasis

Primary tumour formation results from inappropriate and uncontrolled proliferation of cells harboring some form of oncogenic lesion (Hanahan and Weinberg 2000, 2011). These dividing cells are subject to multiple means of tumour suppression to inhibit and prevent tumour development. Some intrinsic factors regulating tumour progression include: genotoxic stress by the oncogenes, growth inhibitory factors, and apoptotic and senescence pathways (Hanahan and Weinberg 2000, 2011). Primary tumours that continue to grow must possess the ability to evade many of these intrinsic suppressive roadblocks to allow malignant progression. Primary tumour cells will also come in contact with extrinsic factors that impede malignant development. For example, the host immune system can mount a response against the tumour or a cut off or limited availability of nutrients and oxygen by a

tumour microenvironment could occur, which would limit tumour progression (Kees and Egeblad 2011; Spano et al. 2012). External cues provided by the tumour microenvironment can also influence how tumour cells grow, colonize and concurrently gain the potential to metastasize (DeNardo et al. 2008; Hanahan and Weinberg 2011).

Metastasis is a very complex process, which involves the growth advantage of a primary tumour cell population and the utilization of surrounding nutrients such as growth factors and blood supply, which leads to metastatic initiation (Mehlen and Puisieux 2006; Chaffer and Weinberg 2011) Metastasis results in newly formed secondary tumours that have left the primary tumour site, entered a means of travel (i.e. the blood circulation, the lymphatic system or have actively moved through surrounding tissues such as the extra-cellular matrix) and have seeded a new location for secondary tumour colonization. The majority of metastatic spread to anatomically distant sites occurs through hematogenous dissemination, i.e. through the blood stream. Many migratory cancer cells that have reached a distant site may even remain dormant for years after metastasis, which often causes relapse, rather than colonization immediately (Chaffer and R. Weinberg 2011).

There is some difference of opinion on how and when tumour cells gain the potential to metastasize, including the hypothesis that certain tumour cell masses possess unique heterogeneity or mixed cell content, which may lead to a particular cell population performing a specific action such as metastasis. For example, the presence of one small group of cells, termed cancer stem cells (CSCs), within a tumour mass, have been shown to exhibit enhanced self renewing properties similar to normal stem cells that are found in the body (Pardal et al., 2003). CSCs have been shown to be capable of giving rise to many of the

malignant cell types from the tumour in which they were initially isolated (Bonnet and Dick 1997, Al-Hajj et al., 2003; Singh et al., 2004). Additionally, very small numbers of CSCs have been shown to be able to generate secondary tumours following transplant experiments in mice (Cho and Clarke 2008). These early tumour-initiating steps of the metastatic cascade are consistently being explored in cancer research to confirm proposed hypotheses and provide further evidence on how tumours form through CSCs mediated initiation (Akhtar, Bussen, and Scott 2009; M. C. Dovey and Zon 2009; Williams 2012).

It is generally respected that the tumour microenvironment in which a cancer cell population is located, may play just as important of a role as the tumour cells themselves, in determining and regulating cancer progression (Hanahan and Weinberg 2011). One common microenvironmental condition that primary tumours are often exposed to is hypoxia. Hypoxia is a form of oxygen deficiency caused by abnormal microcirculation and rapid growth of tumour cells (Miyake et al., 2012). Tumour cells exposed to hypoxic conditions will expand significantly and exhibit decreased susceptibility to undergo apoptosis. Moreover, tumour cells will increase the cellular abundance of hypoxia inducible factor-1 (HIF1) to activate genes that promote angiogenesis, anaerobic metabolism and cell survival (Harris, 2002). HIF1 stabilization has been shown to correlate with metastatic relapse and decreased survival of cancer patients (Semenza 2003). HIF1 is one of several factors belonging to the hypoxia induced factor family, which also includes HIF1 α (Smith et al. 2008). Many solid tumour cells are often immersed in environments with fluctuating or very low oxygen concentrations. These cells in turn can become hypoxic and gain many malignant advantages including resistance to radiotherapy and chemotherapy and enhanced

metastatic capacity (J. M. Brown and Wilson 2004; Chi et al. 2006). Expression of numerous HIF1 target genes, such as vascular endothelial growth factor (VEGF), are induced by hypoxia in many cell types (Semenza 2003). HCT116 colon cancer cells, transfected with HIF1 α 66, have increased expression of VEGF and display markedly high tumour angiogenesis (Ravi et al. 2000). The specific factor HIF1 alpha (α) has been shown to be upregulated by Y-box binding protein (YB-1) in MCF10AT-YB-1 cells (Evdokimova et al. 2009). YB-1 has been shown to upregulated in a variety of cancers (Kohno et al. 2003) however the precise mechanisms by which the multifunctional protein confers or contributes to tumour cell invasiveness remain elusive. YB-1 will be discussed in further detail in section 1.3.

1.2.2 The Metastatic Cascade

There are several mechanisms that tumour cells experience, that characterize a complete metastasis event. It is generally accepted that these steps describe the metastatic cascades of virtually all-migrating cancers. These events include: cell mobility, intravasation, survival and migration through the circulatory and/or lymphatic systems, extravasation and subsequent colonization; after which secondary tumours may undergo periods of dormancy (Figure 2).

In order to metastasize, tumour cells must enter (intravasate) neighbouring, and/or recruited vasculature, to travel to distant sites for presumptive secondary tumour colonization. Hanahan and Folkman provided evidence for an “angiogenic switch” that promotes the development of neovasculature by tumour cells, which aids in providing adequate means for travel (D Hanahan and J Folkman 1996). While the majority of

metastatic transit is observed in blood vessels, the lymphatics provide an alternative route, which may be more easily accessible by a newly disseminated tumour cells. The lymphatic vessels have fewer tight regulated junctions than those observed in the endothelial wall of blood vessels, making them quite leaky. Tumour cells can easily gain access to the lymphatic vessels along with the normal, interstitial fluid, and travel to nearby or distant lymph nodes and subsequently into the hematogenous circulation (Alitalo, Tammela, and Petrova 2005). Breast cancer most frequently metastasizes to regional lymph nodes before traveling to the lungs, liver and bones (Cunnick et al. 2008). By contrast, sarcomas more commonly metastasize directly through hematogenous spread, without disease evidence in the lymphatic vessels or lymph nodes. Matrix metalloproteinase's (MMPs) are active proteases that function in remodeling and degrading the extra-cellular matrix (ECM), which also play an important role in metastatic intravasation. Tumour cells can direct MMPs to degrade the nearby ECM to allow for endothelial cell migration and subsequent tumour angiogenesis. MMPs may also act to create paths through ECM for mobile tumour cells to travel toward local blood vessels for transport (McCawley and Matrisian 2000).

Upon entering the circulatory system malignant cells must be able to endure the internal pressures such as host immune response and the physical stress of travel in the flowing circulation, before they may gain access to virtually all of the organs/tissue within the body. Tumour cells need to avoid the overall stress that comes with their time in transit, as well as avoid immune defenses. Tumour cells in circulation may have increased survival through the co-opting of local blood platelets, which are used as shields to avoid immune responses (Nash et al. 2002).

The next step in metastasis is extravasation; the migration out of the vasculature and into nearby tissue. For osteosarcoma cells, an anchoring protein, called erzin, has been shown to promote migration from the circulation into tissue by facilitating the attachment of osteosarcoma cells to the endothelial cell wall of blood vessels. The inhibition of erzin results in higher rates of osteosarcoma cell death prior to extravasation (Khanna et al. 2004).

Vascular endothelial growth factor (VEGF) has also received recent attention as a potential player in promoting extravasation. When endothelial cells activate internal Src family kinases in the presence of VEGF, can be released from the tumour cells in circulation, they begin to break down their endothelial cell junctions, which may allow the extravasation of tumour cells into tissue (Criscuoli, M. Nguyen, and Eliceiri 2005; Weis and Cheresh 2005).

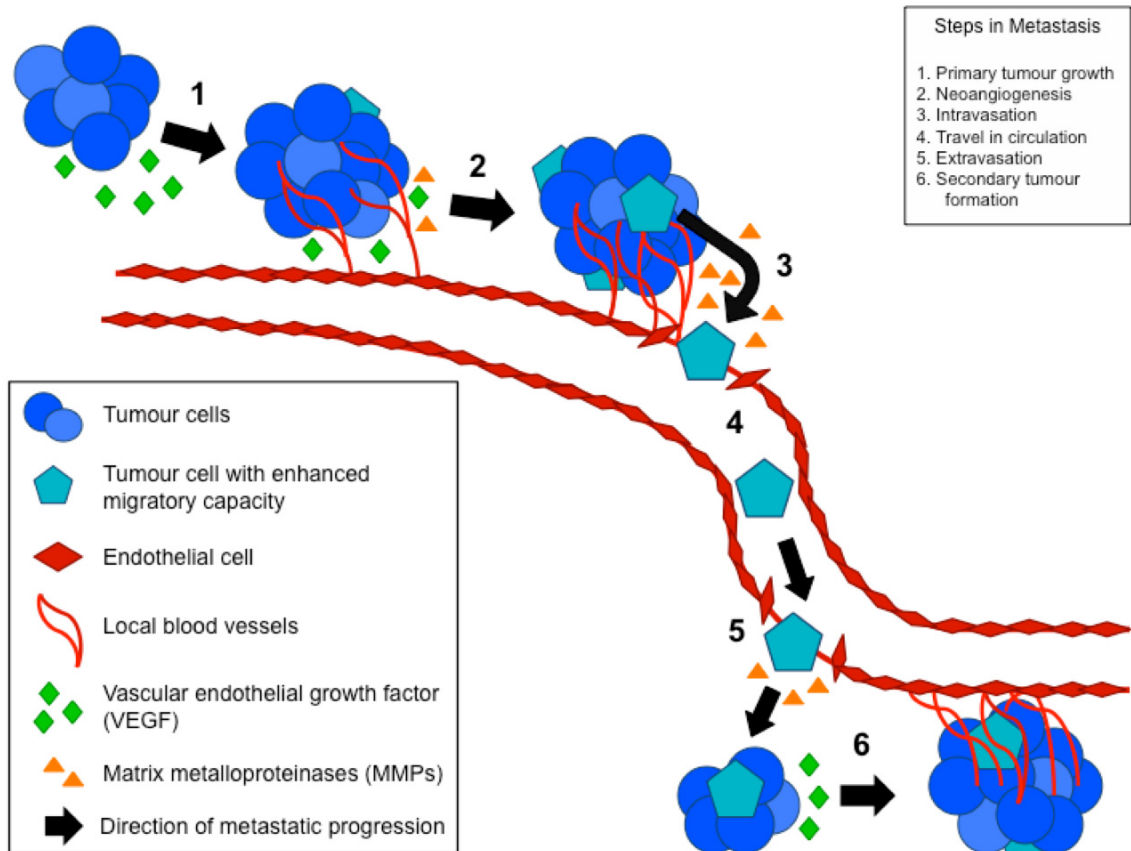


Figure 2. Schematic of the key steps associated with successful cancer cell metastasis.

Following oncogenic transformation, primary tumour cells seek out nearby host vasculature to obtain sufficient oxygen for growth and expansion (1). VEGF is an important growth factor that can be released by tumour cells to induce neoangiogenesis; the new growth or extension of blood vessels from a local parental source (2). As the primary tumour expands specific cell populations may gain an increased capacity to migrate and/or metastasize. These highly migratory tumour cells, with the assistance of local MMPs, which function to degrade and remodel extra-cellular matrix (ECM), can intravasate into the local blood vessels by squeezing through the endothelial cell junctions (3). Tumour cells use the circulatory system as a means for travel (4) until they extravasate out of circulation and into distant tissue (5). At this point tumour cells have the potential to colonize the newly established tissue compartment and form secondary tumours (6). (Chaffer and Weinberg 2011; Hanahan and Weinberg 2011)

From here, tumours cells will need to colonize their newly found tissue regions to establish new secondary tumours. In some cases, tumours may become trapped in smaller capillary beds or intravascular space. If this occurs during a period of tumour growth/expansion it may lead to the rupture of the tumours into the surrounding tissues rather than the migration into these tissues (Al-Mehdi et al. 2000). It was proposed by Paget in 1889 that tumour cells might behave very similar to seeds such that they may only grow or colonize within a particular soil (the organ/tissue location) following metastasis. This seed and soil hypothesis has been used to describe tumour cell homing actions. Breast cancer cells tend to frequently migrate to bone, lungs, liver and the brain; while prostate cancer metastasizes almost entirely to bones. Sarcomas migrate most frequently to other bones and the lungs. These results may provide a case of preferred sites of colonization by tumours as noted by Paget.

Interestingly, not all tumour cells that intravasate and enter the circulatory system have to immediately begin to colonize a new-found site and form secondary tumours (Douglas Hanahan, R. A. Weinberg, and Francisco 2000; Hedley and Chambers 2009). The period from when a tumour has metastasized but not colonized a tissue compartment to the degree of detection is termed dormancy. Often when in a state of dormancy, tumours have equal levels of both proliferation and apoptotic events, occurring within a reasonable small number of tumour cells and undetectable by traditional scans. When a tumour cell population does develop into a secondary detectable tumour, at some interval following the initial diagnosis of cancer, it is referred to as relapse. Many patients at the time of diagnosis

may already have detectable or even undetectable metastases. At initial diagnosis, ~25% of ES patients present with metastases.

1.2.3 Epithelial to Mesenchymal Transition (EMT)

Many primary tumours evolve from epithelial cell morphological origins. As these cancers progress toward increased invasiveness and metastatic capacity they often lose the expression of E-cadherins, which favor static localized cellular position. Cells lose their cuboidal shape and begin to express N-cadherins, characteristic markers for mesenchymal morphology. This loss has been implicated as a key step in epithelial to mesenchymal transition (EMT). EMT is an important developmental process in early embryonic morphogenesis. Mechanistically, EMT involves the ability of cells with epithelial morphology to transform to a more mesenchymal state, while still having the potential to revert/differentiate back to their original state. EMT has been shown to be essential for specific developmental processes including mesoderm formation and neural tube formation by primitive streak migration (Thiery 2002). In recent years this process has received great attention with respects to cancer progression and metastasis. EMT has been shown to confer mobility in various cancer cell populations enabling tumour dissemination and subsequent metastasis. Recently, it has been suggested that tumour cells that undergo epithelial to mesenchymal transition may develop many of the defining features of CSCs including ability for self renewal (Brabletz et al. 2005). This suggests EMT may not only confer increased cellular mobility but also the ability to self renew, which is vital for tumour cells to form secondary tumours following metastasis. It has also been shown that some cancer cells such as carcinoma cells, which go through EMT, may have increased resistance to

apoptosis which in turn allows the population to travel from primary to secondary sites during metastasis with high survivability (Ruth J Muschel and Gal 2008). Several transcription factors have been implicated in regulating EMT including Snail1. Snail1 has been shown to repress the expression of E-cadherins and to be regulated by both NF- κ B and Y-box binding protein 1(YB-1) (Mouneimne and Brugge 2009; Yadi Wu et al. 2009). YB-1 is a recently identified DNA/RNA binding protein that has been shown to suppress cell proliferation and activate transcription factors, such as Snail1, to promote EMT (Evdokimova and Sorensen 2006).

1.3 Y-box Binding Protein

1.3.1 Background

Y-Box binding protein 1 (YB-1) belongs to the cold shock domain family of proteins that have been shown to control various levels of transcription and translation. YB-1 consists of three primary domains: the N-terminal domain, the cold shock domain (CSD) and a C terminal tail. The CSD is a highly conserved region that confers the nucleic acid binding capacity of YB-1 with RNA and single-stranded/double-stranded DNA. Both the N and C terminus are less conserved among Y-box proteins. The charged C terminus of the Y-Box proteins, which contains alternating acidic and basic amino acids, may be responsible for its RNA-binding affinity (Matsumoto and Bay 2005) (Figure 3). Y-box proteins have been shown to exist predominantly in the cytoplasm of a variety of cell types. Given that these proteins also regulate transcription, they are also expected to localize to the nucleus when exposed to certain cellular conditions. UV irradiation, hyperthermia and increased endogenous YB-1 can induce an overall migration or translocation to the nucleus. Y-box

proteins are capable of nuclear-cytoplasmic shuttling, a process by which they are able to move between the two cellular compartments in times of stress, unique to the conserved CSD of the protein. The relative role of transcription versus translation in YB-1 functions remains controversial (Eliseeva et al. 2011).

1.3.2 YB-1 and EMT

The role of YB-1 in cancer/tumour progression has gained attention in the last decade. YB-1 is ubiquitously expressed in various tissues and has been shown to be upregulated in a variety of human cancer including prostate, lung, colorectal, ovarian, thyroid and breast cancer. In 2005, using a transgenic mouse model, Bergmann et al. demonstrated that YB-1 overexpression may lead to breast cancer through the development of genetic instability caused by centrosome amplification and mitotic failure (Bergmann et al. 2005). Extensive literature links YB-1 upregulation to tumour aggressiveness in both epithelial and mesenchymal malignancies (ErbB, Cell, and Cancer 2009; Evdokimova, Tognon, Ng, and Sorensen 2009; Gluz et al. 2009; Ying Wu et al. 2012). Moreover, YB-1 is believed to promote metastasis by a variety of mechanisms including the enhancement of MMPs, which facilitate cell migration (Cheng et al. 2002). It has been demonstrated that YB-1 over-expression induces EMT in human mammary epithelial MCF10AT cells that are transformed prior by activated *H-Ras* (Evdokimova et al. 2009). MCF10AT cells are epithelial cells with cuboidal shape. However, in the presence of increased levels of YB-1, these cells transform into a more mesenchymal morphology, which is associated with increased migratory capacity.

1.3.3 YB-1 and Cell Cycle Regulation

YB-1 is capable of regulating translation of specific mRNA transcripts. YB-1 translationally represses growth-related messages such as cyclin D1 and cyclin E, as well as several cyclin-dependent kinases (CDKs) to block cell proliferation, while translationally activating *Snail1*, *Twist*, and other EMT-associated genes, which are also known to inhibit proliferation and promote a migratory cell phenotype. Cyclins and CDKs are a group of proteins that together, when forming cyclin/CDK complexes, function to control the progression of cells through the phases of the cell cycle (Simmons Kovacs et al. 2008). Induced *Snail1* and *Twist* translation appears to occur through a cap-independent mechanism involving unwinding of 5'-stem loop structures in *Snail1* and *Twist* mRNAs, rather than a cap-dependent mechanisms, which requires the 5' cap recognition by a eIF4F complex to induce translation (Evdokimova et al. 2009). YB-1 acts by binding to the 5' mRNA cap region and displacing/inhibiting eIF4E driven translation initiation (Bader and Vogt, 2005; Evdokimova et al 2006). Translational silencing by YB-1 might be the likely cause of cyclin repression however research is still ongoing to determine the specific mechanisms that regulate the downregulation of cyclins/CDKs and subsequent cell proliferation.

YB-1 has been shown to promote cell cycle progression through a CDC6 dependent pathway in different human cancer cell lines. CDC6 is a regulator of DNA replication within eukaryotic cells. During S phase CDC6 and other pre-replicative complexes such as Cdt1 and Orc1-6 form to initiate DNA replication. When not functioning in S phase, CDC6 is targeted for proteolysis by anaphase promoting complex in. Phosphorylation by CDKs protects CDC6 from proteolysis allowing for S phase entry and activity. Knockdown of YB-

1 by siRNA results in markedly decreased amounts of breast cancer cell populations that are in the S phase of the cell cycle, as well as key cycle regulator cyclin D1 (Basaki et al. 2010). Though reduced expression of YB-1 in a population of cancer cells was also associated with decreased CDC6 expression and subsequent mitotic inhibition, when CDC6 was reintroduced into the cell population, they regained high proliferative characteristics. This finding demonstrates that YB-1 exists upstream of CDC6 to regulate its expression and by ectopic rescue, of CDC6, mitotic activity can be restored. Moreover, CDC6 plays a role in downstream cyclin production following S phase of the cell cycle (Basaki et al. 2010).

1.3.4 The Roles of YB-1 in Multidrug Resistance and Tumour Suppression

A strong correlation between YB-1 overexpression and in multidrug-resistance has been shown in breast, gastric, and pancreatic cancer cell lines. In breast cancer cell lines specifically, YB-1 has been shown to be associated with P-glycoprotein (Pgp). Multidrug Resistant Protein 1 (*MDRI*), codes for Pgp, which causes significant drug resistance for certain cancers (H. Saji et al. 2003). YB-1, when overexpressed, has been shown to promote the transcription of the *MDRI* gene, results in its concurrent elevated expression. These membrane bound proteins are known to confer cellular protection to xenobiotics and drugs, therefore Pgps are a valid molecular target for limiting the chemoresistance that is observed in different forms of cancer when they are treated with chemotherapeutic regimens (Oda et al. 2003). YB-1 has been shown to bind and interact with p53 as well, which may be related to the increased self-defense of cells that are exposed to DNA damaging agents (Okamoto et al. 2000). The tumour suppressor protein, *p53*, functions to stimulate cell-induced apoptosis, DNA repair, and senescence in cells undergoing genotoxic stress and subsequent

genetic alteration. *p53* can induce cell cycle arrest in the G₁, G₂, and S phases of the cell cycle through p21 inhibition of cyclin dependent kinases, as well as, promote Bax mediated cell apoptosis (Bai and Zhu 2006). *p53* is frequently mutated in many human cancers, often inhibiting its biological functions to halt the proliferation of genetically unstable/mutated cells, which allows the formation of primary tumours. (Hanahan and Weinberg 2000; Mehlen and Puisieux 2006).

Along with promoting many forms of cancer, YB-1 is also believed to function to block some pro-oncogenic processes. YB-1 is known to inhibit phosphoinositide 3-kinase (PI3-kinase) and Akt-induced cell transformations by interfering with the synthesis of growth-related proteins such as growth factors and cell cycle proteins associated with the PI3K and Akt pathways (Bader et al. 2003). PI3K and Akt pathways act to promote cancer by increasing overall cell survival by inhibiting a variety of anti-cancer cellular mechanisms including: *p21*, *p53* and pro-apoptotic pathways such as Bax related, stress induced, apoptosis (Hanahan and Weinberg, 2000; Croce 2008).

Y-box protein

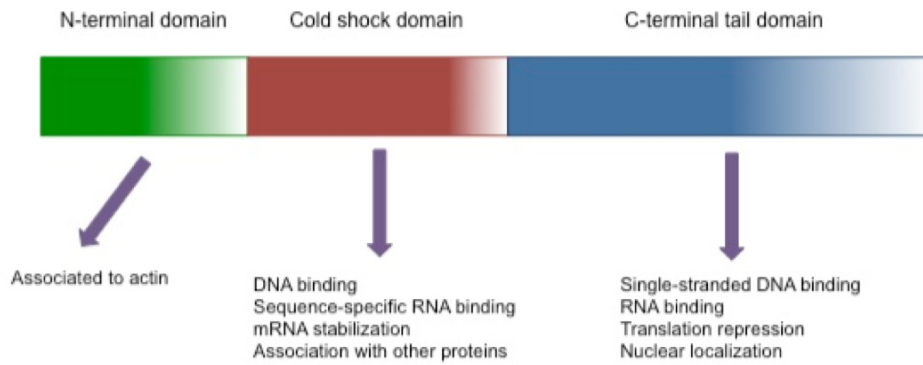


Figure 3. Diagram of the general structure of Y-box binding proteins. Some of the known functions of each protein region are noted with purple arrows (Modified from Matsumoto & Bay 2005).

1.3.5 YB-1 and *EWS-FLII* in Ewing's sarcoma

YB-1 has been specifically shown to play a role in the splicing of pre-mRNA through cooperate RNA polymerase II binding with translocation liposarcoma protein (TLS) and EWS. Chansky et al demonstrated that in ES cells, the presence of endogenous expression of common ES *EWS-FLII* fusion protein inhibited YB-1 recruitment to RNA polymerase II. These results suggested that *EWS-FLII* fusion proteins might play a role in promoting malignant transformation in ES, through a loss of function of YB-1 protein assisted splicing (Chansky et al. 2001). It is possible that *EWS-FLI*- mediated inhibition of YB-1 recruitment to the nucleus, may make YB-1 more abundant in the cytoplasm, which may lead to an increase in post-translational modification activity of YB-1 resulting in overexpression of EMT-associated messages including *Snail1*, *Twist* and *HIF1 α* . The Sorensen laboratory conducted preliminary *in vitro* studies on YB-1 in ES cell lines and demonstrated that by reducing YB-1 levels, cell migration was concurrently reduced. (Figure 4). These observations lead to the need of further studies to be conducted in animal models for confirmation of the phenotypes.

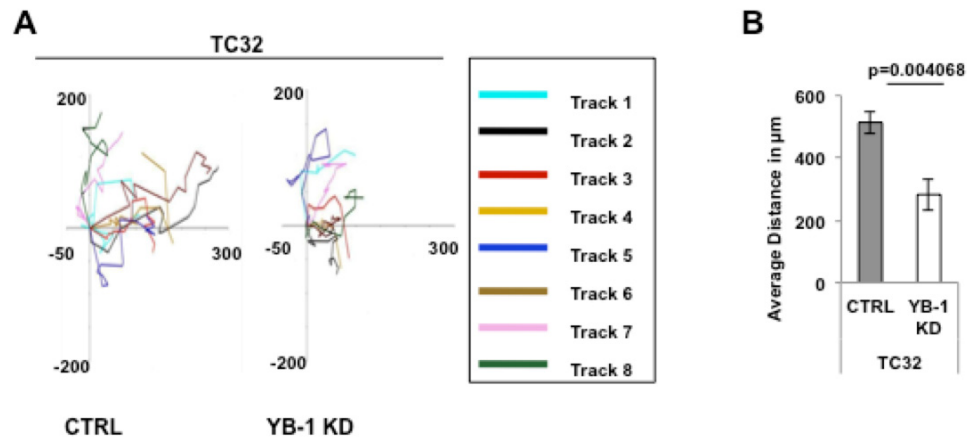


Figure 4. *In vitro* migratory behaviour of both TC32 ctrl and TC32 YB-1 kd cells.

TC32 cells were grown to 80% confluency then scratched near the middle of the tissue culture plate and followed over a 20 h period. Using fluorescent microscopy cells were imaged at 1h intervals to monitor their attempt to close the wound edge. Images were then analyzed using Velocity software. Eight cells, of each of CTRL or YB-1 KD TC32 cells were randomly chosen from the wound edge and their paths were tracked. X- and Y-axis migration plots, of each cell were generated as well as the average total length of tracks for each cell line was determined and expressed in μm (A). TC32 CTRL cells display a greater average distance traveled compared to YB-1 KD cells (B). CTRL = TC32 cells injected with control shRNA; KD = TC32 cells injected with YB-1 shRNA Figure provided by Amal El-Naggar, Sorensen Lab 2011.

1.4 Zebrafish as a Cancer Model

1.4.1 Zebrafish Background

Zebrafish, *Danio rerio*, (Figure 5) are small tropical fish originating from the Ganges River, and surrounding bodies of water, of India and Burma. The zebrafish first emerged as a valuable model system for studying development processes in the 1960s (Streisinger et al. 1981). The zebrafish began being used as a model for cancer when it was used to determine the effects of certain carcinogens. Water-soluble carcinogens can be added directly to fish water and induce tumour formation in zebrafish (Okihira and Hinton, 1999; Beckwith et al., 2000; Amatruda et al., 2002; Berghmans et al., 2005a; Mizgireuv and Revskoy, 2006). These chemically induced tumours display histological and molecular similarities to human malignancies including high proliferation rates, low degrees of cell differentiation and an overall resemblance in the gene signatures involved in regulating DNA damage/repair, cell cycle progression and apoptosis (Lam and Gong, 2006). A combination of chemical carcinogenic, mutant lines, transgenic lines and xenograft models, each with their own advantages and disadvantages, are currently being utilized to study human cancers (Table 1).

Zebrafish and other teleost fish are known to develop tumours spontaneously, which have strikingly similar molecular and histopathological features to those observed in human disease (Feitsma and Cuppen 2008; Stoletov and Klemke 2008; Liu and Leach 2011). The zebrafish has a number of advantages as a developmental model: (1) they share 85% genetic similarity to humans, (2) low cost for animal maintenance, (3) rapid external development, (4) optically transparency, and (5) the availability of transgenic

Table 1. Zebrafish cancer models (Modified from Stoletov and Klemke 2008)

Model Type	Primary Function	<i>In vivo</i> imaging	Advantages	Disadvantages	References
Chemical carcinogenesis	To evaluate carcinogenic activity of chemical compounds or mutant fish lines with developmental abnormalities	Low magnification of tumours in living fish. High magnification of fixed specimens	Easy to perform and no need of specific zebrafish strains	Delay of onset and incidence of tumour formation.	Okiihiro and Hinton 1999; Amatruda et al. 2002; Lam and Gong 2006
Mutant lines	To screen for genetic or chemical factors that promote tumour formation	Low magnification of tumours. High magnification of fixed specimens	Fairly short onset of tumour formation.	Need to develop/use specific fish lines	Amsterdam et al. 2004; Berghmans et al. 2005b; Shepard et al. 2005
Transgenic lines	To study tumour initiation/progression and visualize specific zebrafish cell components (immune cells)	Fluorescently tagged transgenes enable high resolution imaging	High incidence of tumour formation, ability to induce and control initiation of a specific tumours	Need to develop/use transgenic lines which may be genetically unstable	Langenau et al. 2003, 2007; Patton et al. 2005; Yang et al. 2004
Xenograft (30 days post fertilization)	To study tumour cell-zebrafish microenvironment interactions	Fluorescent tumour cell labeling enables high resolution imaging	Many fish can be injected at once, number, type and location of injected cells is controlled. All organs are developed	Immunosuppression necessary, tumour may survive in fish for a few weeks only	Stoletov et al. 2007
Xenograft (2 days post fertilization)	To study tumour cell-zebrafish microenvironment interactions	Fluorescent tumour cell labeling enables high resolution imaging	Many fish can be injected at once, number, type and location of injected cells is controlled. No immunosuppression necessary	Injected tumour cells may only survive for a few weeks. Many major organ systems are still developing/growing	Please refer to Table 2 (Page 37).

and mutant lines. These attributes combine to make the zebrafish a promising and effective animal model for studying cancer. Zebrafish reach sexual maturity at approximately three months of age and are capable of producing upwards of two to three hundred offspring (embryos) per mating pair. Eggs from female fish are fertilized externally, which allows for easy access for genetic manipulation (Detrich, Westerfield and Zon, 1999).

1.4.2 Implications for Using Zebrafish to Study Cancer

The zebrafish has emerged as a powerful model system for studying human cancer (Berghmans et al. 2005; D. M.; H. W. Yang et al. 2004). Many of the oncogenes and tumour suppressor genes, identified as important players in human malignancies, have zebrafish homologues, and the critical pathways regulating cell growth, proliferation, apoptosis and differentiation appear well conserved (Feitsma and Cuppen 2008; Payne and T. Look 2009; Stoletov and Klemke 2008; Liu and Leach 2011). The development of transparent fish strains such as the wholly transparent mutant zebrafish *casper* (R. M. White et al. 2008), coupled with advanced *in vivo* imaging technologies and procedures, has allowed the zebrafish to emerge as a novel and versatile model system for unraveling the underlying mechanisms associated with human cancer development and disease progression, including metastasis.

Many of these zebrafish cancer models have utilized the power of genetic manipulation to develop transgenic lines that express mammalian oncogenes. Zebrafish transgenesis involves introducing foreign DNA into the genome of one-cell stage embryos and having it subsequently become expressed in the cell or tissue population of interest. Using tissue specific promoter regions to drive gene expression, transgenic zebrafish can be

used to study the initiation and/or the progression of specific cancers. Langenau et al. 2003 published the first transgenic model of human cancer, T-cell acute lymphoblastic leukemia (T-ALL), by overexpressing *c-myc*, an oncogene with a dual function in cell proliferation and apoptosis, under the zebrafish T-cell specific *rag2* promoter. These zebrafish displayed rapid onset of T-ALL as early as 21 days post fertilization (dpf) (D. M. Langenau et al. 2003). Subsequently, several other transgenic zebrafish models of lymphoblastic and myeloid leukemia have been generated, including a model of high risk acute myeloid leukemia caused by the t(7;11) NUP98-HOXA9 translocation by our laboratory (Forrester et al. 2011)

Transgenic models of solid tumours have also been generated. In one study, overexpression of activated human RAS, a common mutation in a variety of human cancers, was put under the control of a β -actin promoter, and resulted in the formation of several different tumours in zebrafish including peripheral nerve sheath tumours and rhabdomyosarcomas (Le et al. 2007). Langenau et al. 2007 developed a zebrafish model of embryonic rhabdomyosarcoma (ERMS) by overexpressing human activated RAS (kRASG12D), under the *rag2* promoter. Half of all injected embryos developed ERMS within an 80 dpf interval of observation (D. M. Langenau et al. 2007). Tumourgenesis accelerated exponentially when these experiments were conducted using a *tp53* mutant zebrafish line (Berghmans et al. 2005). Melanomas can also be studied in zebrafish using transgenic zebrafish lines expressing mutated *BRAF* in melanocytes. Human melanomas commonly have mutations in *BRAF*, a gene associated with regulating cellular growth through B-Raf proteins. Zebrafish with mutated *p53* (Berghmans et al. 2005) and *BRAF*

develop large lesions of proliferating melanocytes (Patton et al. 2005). Most relevant to my research Leacock et al developed a transgenic zebrafish expressing the *EWS-FLII* fusion oncoprotein under a zebrafish heat shock promoter. Following heat shock, these transgenic fish developed tumours with similar histology to that of human ES that could be serially transplanted into irradiated zebrafish recipients and displayed successful ES engraftment and tumour formation within three to five weeks. However, the incidence of fish developing these tumours spontaneously due to the expression of *EWS-FLII* was relatively low and developmental abnormalities such as stunted embryo growth were also observed (Leacock et al. 2012).

1.5 Zebrafish Xenotransplantation

Xenotransplantation is the transfer of one species-specific tissue (xenografts) to a new animal species and has been utilized as a tool for many years in cancer biology (Cariati, Marlow, and Dontu 2011; Johnson et al. 1995; Merk et al. 1972). Xenograft experiments have been extensively performed in mouse models of human disease enabling the analysis of cancer cell proliferation, invasion, migration and induction of growth advantages such as increased angiogenic recruitment (Cheon and Orsulic 2011). While transgenesis has been a traditional approach to modeling human malignancies in zebrafish (Chen and D. M. Langenau 2011; Leacock et al. 2012; Project et al. 2005) more recently, the xenotransplantation (XT) of several human cancer cell lines has been successful. Zebrafish offer a cancer research platform with superior imaging capabilities based on size and transparency of both wildtype embryos and mutant fish.

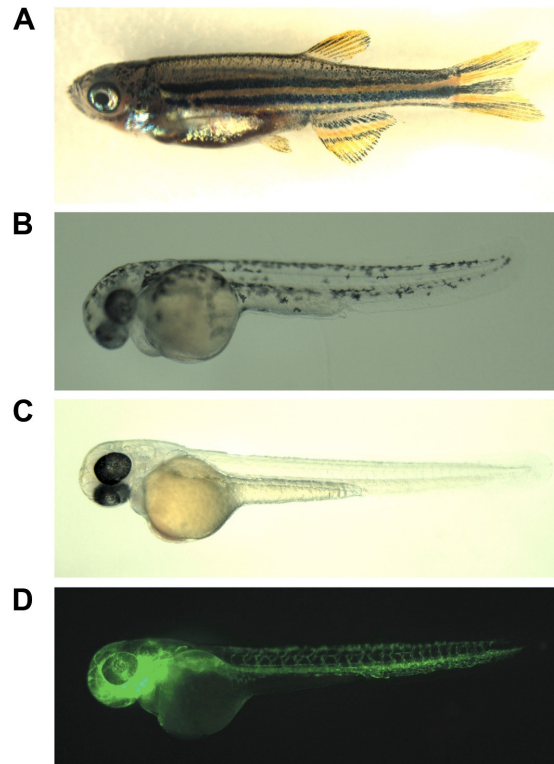


Figure 5. Wildtype (wt) and select mutant zebrafish lines. This figure displays an adult wt AB strain zebrafish (A), an approximately 28 hours post fertilization (hpf) wt AB embryo (B), a 48 hpf transparent mutant *casper* embryo (White et al., 2008) (C) and a 48 hpf *tg(fli1a:eGFP)* (Lawson and Weinstein 2002) *casper* embryo (D) with labeled vasculature. The most common embryo line used for the research presented in this thesis is the *casper* line. Panel developed by: Andrew Coombs and Angela Young of the Berman Laboratory.

Moreover, a large number of recipient embryos can be produced, due to the high fecundity of the adult zebrafish. The zebrafish is highly amenable to live cell analysis of the tumour-microenvironment interactions *in vivo*, which when coupled with superb cost effectiveness makes the zebrafish an attractive model for uncovering, observing and studying specific mechanisms in cancer progression including metastasis. Thus, zebrafish offer unique opportunities to further explore the use of xenotransplantation in the study of human cancers.

Lee et al., 2005 demonstrated that human melanoma cells could be injected, survive and have the ability to migrate in the zebrafish. Melanoma cells were injected into the blastula stage of zebrafish embryos and their behaviour was observed over the following days. Lee et al showed that these cells could be tolerated within the zebrafish for at least eight days post injection and would home to the epidermis of the embryos - the natural site for human melanoma cells. These results suggested that zebrafish may possess homing cues and/or signals that are conserved and can be interrupted by the injected human melanoma cells. Human fibroblasts and normal healthy melanocytes were also injected into zebrafish and displayed similar survivability to that of the melanoma cells, but lacked the migratory capacity. This study was one of the first xenotransplantation studies to demonstrate the utility of the zebrafish as a cancer model organism for the study of human cancer cell interactions within an *in vivo* tumour-microenvironment.

Recent studies have further developed and optimized the parameters for transplanting human cells in to zebrafish embryos and sequentially analyzing the transplanted recipients (Corkery, Dellaire, and J. N. Berman 2011; Haldi et al. 2006; L. M. J. Lee et al. 2005;

Marques et al. 2009). Many of these xenotransplantation studies were performed to date have used 48 hours post fertilization (hpf). This developmental time point was considered the optimal stage for injection (Table 2). Other advantages apparent in transplanting human cancer cells in 2-5 day old (48-120 hours post fertilization) embryos include large number of animals that can be produced, injected and housed simultaneously, well controlled injection sites that are easily visualized and immunosuppressed zebrafish that have yet to fully developed complete innate and/or adaptive immunity (S. Lam et al. 2004).

Immunosuppression is required for xenotransplantation studies in zebrafish over 30 dpf when adaptive immunity is fully established (S. Lam et al. 2004). All of these characteristics enable the completion of multiple statistically robust experiments simultaneously and the ability to inject foreign cancer cells into an animal without transplant rejection or need for immunosuppression. Though the lack of an immune response is beneficial for initial transplantation and injection, it may become a limitation when observing the interactions taking place in the tumour microenvironment. As observed in human cancer patients, varying immune cell responses may play vital roles in promoting or inhibiting the progression of cancers, as well as the effects of certain cancer treatments (Gupta and Massague 2006; DeNardo et al. 2008; Kees and Egeblad 2011; Spano et al. 2012). Moreover, because foreign tissue and cells are being introduced into fish, it is not certain that all of the molecular mechanisms associated between the recipient and the xenograft will be completely conserved, which may impact cancer cell-xenograft interactions. To date zebrafish xenograft experiments have proven very promising in displaying similar cancer phenotypes, with genetically conserved/shared mechanisms, that are observed in human patients.

Of the several sites of injection the yolk sac was determined to be one of the most optimal anatomic locations due to its size and ease of transplantation (Haldi et al. 2006). 50-100 cells are most frequently utilized to ensure adequate cell survival, proliferation and invasion. The standard incubation temperature for zebrafish embryos and adult fish is 28 °C while the standard temperature for most traditional cell culture is 37°C. A reasonable compromise of temperature for zebrafish embryos transplanted with human cells was found to be 35°C. At this incubation temperature, no evident developmental harm is caused to the embryos and the injected human cells still possess the ability to survive and proliferate *in vivo* (Haldi et al. 2006). Subsequent work has demonstrated that xenografted primary human tumours, such as gastric cancers and primary leukemia, derived from human leukemia patients, can be injected and will proliferate and disseminate, throughout the embryo (Marques et al., 2009; Berman Lab, unpublished data).

In collaboration with the Dellaire laboratory, the Berman laboratory has pioneered xenotransplantation (XT) of human leukemia cell lines into two-day-old *casper* mutant zebrafish embryos. Using a rapid and novel *ex-vivo* proliferation assay, we were able to quantify the cellular proliferation rates for liquid tumours, chronic myelogenous leukemia (CML; K562 cell line), and acute promyelocytic leukemia (APL; NB4 cell line) as well as solid tumours, such as, MCF7 and MDA-MB-231 breast cancer cell lines. These breast cancer cells displayed differential dissemination and migratory behaviour upon XT, suggesting the zebrafish platform could be used to investigate cancer cell migration. Moreover, we were able to specifically inhibit leukemia cell proliferation using drugs that specifically target unique molecular abnormalities present within each of cell line. Imatinib mesylate targets the BCR-ABL fusion protein in K562 cells and all-trans retinoic acid

(ATRA) targets the PML-RARA fusion protein in NB4 cells (Corkery, Dellaire, and J. N. Berman 2011). We have demonstrated that the zebrafish XT model together with the *ex vivo* proliferation assay, has the ability and sensitivity, to detect the effects of target drugs on specific leukemias. These results validate the use of xenotransplantation as an innovative platform for chemical screening in zebrafish embryos with proliferative response as a readout.

While the mouse remains the standard and most commonly used animal model in pre-clinical studies, its ability to be utilized as a platform for rapidly screening for the efficacy of new drugs is ineffective due to the biologic complexity and prohibitive costs associated with these types of assays in mice. The zebrafish XT presents *in vivo* animal model system that is more rapid, cost-effective and amenable to high-throughput drug assays than the mouse. The ability of the XT model to respond to specific tumour-drug interactions positions the zebrafish as a powerful tool to discover novel anti-proliferative and anti-cancer agents through high throughput drug screens.

Table 2. Human cancer cells that have been transplanted into 48 hours post fertilization zebrafish (Modified from Martina et al. 2012)

Tissue/Cell line(s)	Location	Number of injected cells	Cell labeling technique	Reference
Melanoma cell line WM-266-4 Colorectal cancer cell line SW620 Pancreatic cancer cell line FG CAS/Crk Fibroblast cell line CCD-1092Sk	Yolk sac, Hindbrain ventricle, Circulation	50-200 cells	Cells labeled with cell tracking dye	Haldi et al. 2006
Breast cancer cell line MD-MB-435 Ovarial carcinoma cell line A2780	Yolk sac (close proximity to the duct of cuvier)	1000-2000 cells within matrigel	Cells contain transduced fluorescent reporter construct	Nicoli et al. 2007
Breast cancer cell line MD-MB-231	Yolk sac	500 cells with matrigel	Cells contained transduced fluorescent reporter construct or were labeled with tracking dye	Harfouche et al. 2009
Breast cancer cell line MD-MB-231 Ovarial carcinoma cell line OVCAR8	Perivitelline cavity	100-500 cells	Cells labeled with cell tracking dye	Lee et al. 2009
Pancreatic tumour cell lines PaTu-S and PaTu-T Cells of primary pancreatic tumours	Yolk sac	200 cells or tissue fragments/ dissociated cells	Cells labeled with cell tracking dye	Marques et al. 2009
Pancreatic tumour cell lines PaTu-S and Panc-1	Yolk sac	1000-2000 cells	Cells labeled with cell tracking dye	Vlecken and Bagowski 2009
Leukemia cell lines K562 and NB-4	Yolk sac	200 cells	Cells labeled with cell tracking dye	Corkery et al. 2011
Prostate cancer cell line PC3	Yolk sac	~100 cells	Cells contain transduced fluorescent reporter construct	Ghotra et al. 2011
Ovarial carcinoma cell line OVCA- 433	Yolk sac	~100 cells	Cells contain transduced fluorescent reporter construct	Latifi et al. 2011
Breast cancer cell line MD-MB-231 Prostate cancer cell line PC3	Duct of cuvier	40-400 cells	Cells contain transduced fluorescent reporter construct	He et al. 2012

1.6 Rationale

New animal models to study metastasis are vital to discover and develop alternative ways and therapeutics to treat this form of detrimental cancer spread, which is associated with 90% of all cancer related deaths in general. ES patients have a significantly reduced survival when they present with metastatic spread at the time of diagnosis and when they develop metastases at a later time point (Bernstein et al. 2006; Ludwig 2008; Balamuth and Worner 2010). Currently, there are no specific treatment regimens for metastatic ES that have significantly improved patient survival. Moreover, we currently do not have a viable animal model of ES metastasis that can (1) be used to better understand the molecular mechanisms of ES metastasis and (2) investigate and screen for drugs that might act to inhibit ES cell proliferation/metastasis/survival.

I hypothesize that ES cells can be effectively introduced into the zebrafish XT platform and that they will exhibit common invasive and metastatic behavior, in keeping with what is observed in human patients. I also hypothesize that by knocking down YB-1 levels in ES we will observe a reduction in metastatic capacity/migration.

Given that YB-1 has been shown to be up-regulated in a variety of cancers compared to normal tissue counterparts including ES, along with the specific studies that have been conducted on YB-1 promoting EMT in breast cancer, we aimed to investigate whether or not similar invasive mechanisms orchestrated by YB-1 were being employed by ES cells that could subsequently result in metastasis. YB-1 and concurrent downstream translational factors may be conferring metastatic capacity to ES.

The goal of my research project was to use the zebrafish xenotransplantation platform to study Ewing's sarcoma (ES) migration and investigate the role of Y-box binding protein 1 (YB-1) in the metastatic behaviour of ES.

Chapter 2: Methods

2.1 Zebrafish Husbandry & Housing

Zebrafish (*Danio rerio*) were maintained according to standard protocols (Westerfield, 1995). Translucent *casper* mutant (R. M. White et al. 2008)(provided by the Zon Laboratory, Children's Hospital, Boston, MA) and tg(*fli1-eGFP*) transgenic *casper* zebrafish (gift of the look Laboratory, Dana-Farber, Boston, MA) embryos were employed to permit real-time analysis of cancer cell microenvironment interactions without any auto-fluorescence that might interfere with image quality. Embryos were dechorionated using 10 mg/ml stock solution of Pronase (Roche Applied Science). During the xenotransplantation experiments embryos were housed in a 35°C incubator as compromised in order to permit the normal growth and development of the zebrafish embryos, as well as the injected cancer cell line(s) (Lee et al. 2005; Haldi et al. 2006). Use of zebrafish in this study was approved by the Dalhousie University Animal Care Committee, under protocol # 11-132 (Expiry, 2012).

2.2 Cell Line

TC32 cells are a ES cell line with a balanced t(11;22) (Szuhai et al. 2005) common in 85% of disease (provided by the Dr. Poul Sorensen (BC Cancer Agency, Vancouver)). Two versions of this TC32 cell line were employed in my studies: TC32 cells in which YB-1 was knocked down using short hairpin RNA (shRNA) introduced by lentiviral transduction and TC32 cells injected with a control shRNA. Cells were plated 24 hours prior to transduction in 12-well plates. On second day, at approximately 50% confluence, cells were transduced

with either control ready-to-use shRNA lentiviral particles (Santa Cruz Biotech., sc-108080), or ready-to-use YB-1 shRNA human lentiviral particles (Santa Cruz Biotech., sc-38634-V) following the manufacturer recommendations. Selection of stable clones expressing the shRNA was performed using Puromycin selection (Santa Cruz Biotech., sc-108071).

2.3 Cell Preparation and Labeling

For *in vivo* zebrafish studies, TC32 control (ctrl) cells and TC32 YB-1 knockdown (kd) cells were stained with CM-DiI (red fluorescence, Invitrogen). Cells were grown to approximately 80% confluency in RPMI Media 1640 (Gibco) with 10% fetal bovine serum (Gibco) and 1% antibiotic anti-mycotic (Invitrogen), and trypsinized with ethylenediaminetetraacetic acid (EDTA). Cells were washed with RPMI, transferred to 15 ml Falcon tubes and centrifuged for 5 min at 100 X g. Cells were re-suspended at a concentration of 10 million cells per ml in 1X Phosphate Buffered Saline (PBS) (Gibco) with a 5 µg/ml final concentration of CM-DiI. The suspension was incubated for 4 min at 37°C and then for 15 min at 4°C as previously described (Corkery et al., 2011). Cells were washed once in 1X PBS before being suspended in RPMI for injection into embryos. All centrifugations were performed using a IEC Centra CL2 centrifuge (Thermo) (Figure 6).

2.4 Xenotransplantation

48-hour post fertilization (hpf) *casper* embryos were dechorionated and anesthetized with Tricaine (Ethyl 3-aminobenzoate methanesulfonate salt, MS-222, Sigma-Aldrich) at a final concentration 200 µg/mL prior to injection. A manual PLI-100 microinjector (Medical Systems Corp, Greenvale, NY) was used to load the cell suspension into a pulled capillary needle for embryo injection. Embryos were arrayed in a six lane agarose plate prepared in a

medium size (10 cm) Petri dish. Approximately 50 - 100 TC32 cells were injected into the yolk sac of each embryo. Following injection embryos were kept at 28°C for 30 minutes and then re-located to a 35°C incubator for the duration of the experiments. At 12-24 hours post injection (hpi), embryos were screened for the presence of a fluorescent cell mass within the yolk site. Positive embryos were isolated for experiments.

2.5 Live Cell Microscopy and Cell Proliferation Quantification

Every 24h for approximately 168 hpi (7 days) a group of 4-6 embryos, housed in a 6-well plate, were imaged and analyzed for cellular interactions within the zebrafish embryonic microenvironment. An inverted Axio Observer Z1 microscope equipped with a Colibri LED light source (Carl Zeiss, Westlar, Germany) and an AxioCam Rev 3.0 CCD camera and Axiovision Rel 4.0 software (Carl Zeiss Microimaging Inc.) was used to screen, observe and to capture images of injected embryos. Brightfield and accompanying fluorescent images, of both the head and tail regions, were captured for analysis. Each single image frame corresponds to ~1.8 mm in length. The majority of embryos were approximately 3.5 mm in length from 48-168 hpf.

To determine rate of cellular proliferation *in vivo* positively injected embryos were placed into groups of 15-20 embryos and euthanized by a Tricaine overdose at the time intervals: 24 hpi and 96 hpi. Embryos were placed in a microtube of 1.5 ml of pre-warmed protease solution (0.25% trypsin, 1mM EDTA and 45 ml 1X PBS). To this mix, 27µl of collagenase (Sigma-Aldrich, Oakville, ON, Canada) at 100mg/ml was added. Embryos were incubated and undisturbed for 15 minutes. From 15 minutes onward, the embryo-dissociation mix was homogenized using a Pasteur pipette by passing the dissociating

embryos through the pipette and then quickly forcing them out against the bottom of the microtube. This step was repeated as necessary until visual inspection of the microtube revealed fully dissociated embryos. A complete dissociation was confirmed, through personal inspection, by no detectable whole embryo bodies or tissues remaining intact in the cell suspension, with the exception of the spines and eyes of embryos. The duration of the dissociations was approximately 45 minutes. Upon completion, 600 μ l of STOP solution (30% FBS, 6mM CaCl₂, PBS, 6 ml sterile water) was added to the microtubes to end the enzymatic reactions occurring between the dissociation mix and the embryo suspension. The suspension was then centrifuged at 400 X g for 5 minutes and the supernatant removed, leaving approximately 100 μ l of liquid containing the pelleted suspension content containing the single cells produced by the dissociation assay. These cells were washed once in chilled 1X PBS and finally re-suspended in 10ul per embryo of PBS-FBS solution for overnight storage. After 24h the dissociations were analyzed using the inverted Axio Observer Z1 microscope. One 10 μ l drop of the suspension at a time was added to a microscope slide to create a hanging bolus. Boluses were analyzed as a mosaic 4 X 5 grid, using a 5X objective that captured the entire circumference of the bolus. The mosaic capture program compiled equally sized square composite images that represented the entire circular bolus. Following capture, all individual images from the mosaic were analyzed using a semi-automated macro (Image J computer software, NIH, Bethesda, MD, USA) where relative fluorescent cell numbers could be determined per embryo. Of the 20 individual images produced by the mosaic program, 4 out of 6 of the internal/grid images were used to determine cell counts. Exterior grid images were excluded from analysis because they only displayed the circular edge regions of the suspension bolus. Experiments were completed in triplicate

approximately two – three weeks apart (Corkery et al. 2011).

2.6 Cell Migration Assay

To quantify cellular migration, groups of 25-40 embryos were followed from 24h - 144h using live cell microscopy of the tail region and compared to the anterior dissemination in the head region. I decided to employ a predetermined anatomic region of the zebrafish embryo from the cloacae to the tip of the tail, as the region to evaluate, for migration. Embryos were scored based on the presence or absence of fluorescent cells within the tail tissue. By convention, embryos displaying six or more cells within the tail region were scored positively for migration. The embryos that were scored negatively for a particular day of experimentation were re-examined on the days following to confirm presence or absence of cellular migration overall by the final time interval 120 hpi, used to determine statistical significance of migratory results between groups. TC32 cells fixed in 4% paraformaldehyde and TetraspeckTM microspheres were employed as negative migratory controls (Figure 7).

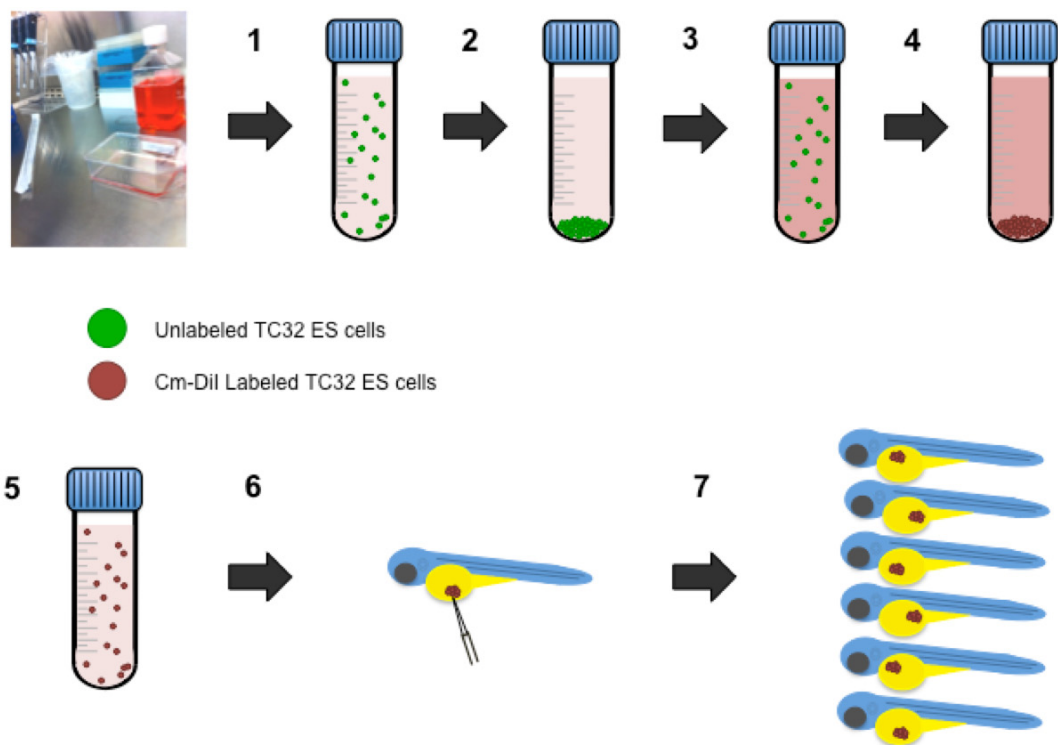


Figure 6. Overview of XT cell labeling and injection procedures. Unlabeled TC32 ES cells (green) are trypsinized in a standard 75ml tissue culture flask (1) and centrifuged into a pellet (2). The pellet is re-suspended into a Cm-DiI dilution (3) and incubated for 5 minutes at 37°C and 15 minutes at 4°C, resulting in successful cell labeling with fluorescent Cm-DiI (4). At a suspension of approximately ten million cells per ml (5), labeled TC32 cells (red) are injected into 48 hours post fertilization (hpf) *casper* embryos (6). 50-100 cells are injected into a single embryo. Successfully injected embryos display a fluorescent mass in the yolk sac and are pooled for simultaneous experiments (7).

2.7 Statistical Analysis

IBM SPSS 17.0, Statistical Package for the Social Sciences, software was used to determine relative risk, odds ratios and overall statistical significance of the null hypothesis displayed by chi-squared analysis of all migration data sets. Chi-squared tests were conducted on my dataset because only one variable was being analyzed at a time (e.g. the presence or absence of cell migration to the embryo tail). Contingency tables were developed for both TC32 cell vs. Fixed TC32 cell migration (Appendix A) and TC32 ctrl cell vs. TC32 YB-1 kd cell migration (Appendix B). Using these two by two contingency tables, expected values of migration due to chance alone, and Pearson chi-square values were determined for each experimental group. P-values less than 0.05 implied significant relation. Errors bars for all figures represent ± 1 standard deviation (SD).

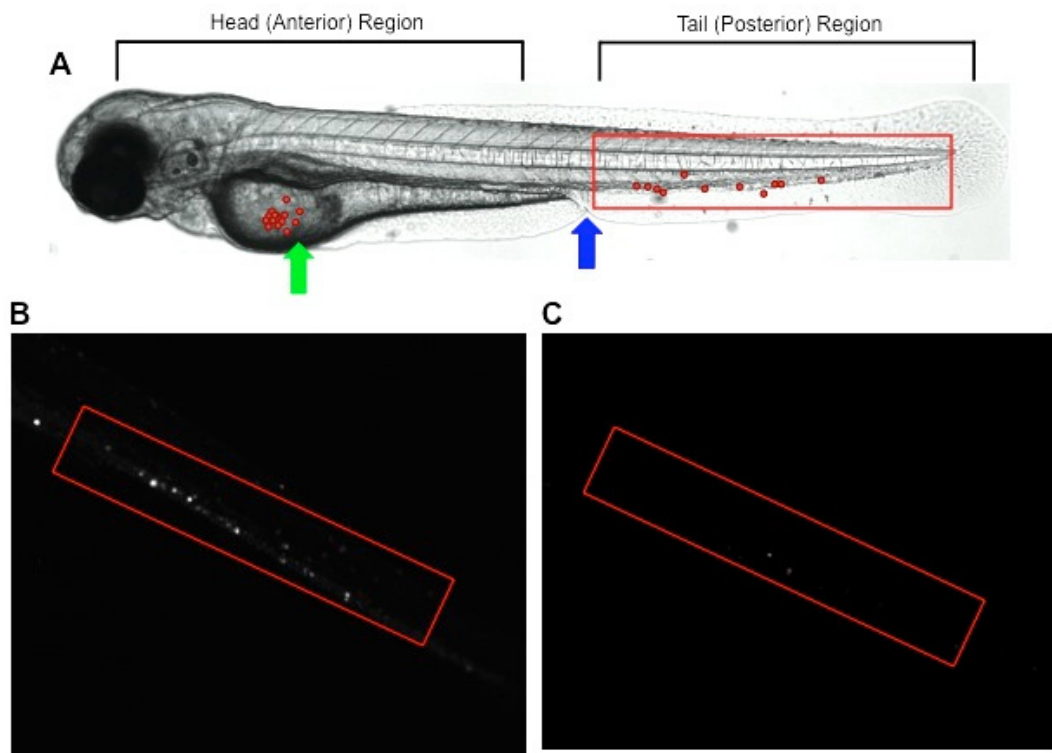


Figure 7. Anatomic regions of the zebrafish XT model and scoring scheme for cell migration assay. The primary site of all Cm-Dil labeled cellular injection is the *casper* zebrafish embryo yolk sac shown with a green arrow (A). Cells are shown as red circles. Scoring of migration was conducted within a predetermined area between the cloacae and the posterior tip of the tail tissue. Any embryo displaying six or more fluorescent cells in the region encompassed by the red outlined box, was deemed a positive migratory phenotype (B). Embryos that showed less than six cells were deemed negative (C). Migratory analysis was conducted every 24 h starting at 24 hpi until 120 hpi. Cells appear as white circles in 2 dimensions under a 555 nm excitation filter. Approximately, 25-40 embryos were used in each migration experiment (hpi = hours post-injection).

Chapter 3: Results

3.1 TC32 ES Cell Lines Survive and Proliferate in Zebrafish Embryos.

Given our laboratory's prior successes with the xenografting of both liquid (leukemia) and solid (breast cancer) tumour cell lines, my first goal was to develop and optimize an approach to inject ES cells into our established zebrafish XT model. TC32 ES cells were efficiently introduced into 48 hpf *casper* embryos (Figure 8). The fluorescent cellular signal, emitted by the covalently bound Cm-DiI, enabled the tracking of these cells *in vivo* to determine their behaviour within the zebrafish microenvironment. Through several trials it was determined that 50-100 cells was the optimal cell number for injection. Less than 50 cells resulted in poor numbers of positively injected embryos that could be used for experimentation. Greater than 50 cells lead to mortality of many embryos, as well as the methodological need for increased injection accuracy in attempt not to unintentionally inject or force cells into the vasculature within the yolk sac. The injected masses of 50-100 cells were easily visualized as a dense fluorescent ball or bolus present within the approximate center of the embryonic yolk sac at 24 hours post injection (hpi). Cellular dissemination in the anterior (head) region of the embryos was observed as early as 48 hpi and continued throughout individual experiments. Cellular proliferation was quantified using our published *ex vivo* proliferation assay (Corkery et al. 2011). Compared to *in vitro* proliferation rates, *in vivo* proliferation rates of TC32 cells were determined to be slower (Figure 9). The time it took for overall cell numbers to double *in vitro* was 48 h while *in vivo* cell numbers doubled at approximately 72 h, displaying a 24h discrepancy in proliferation between the two systems. This difference may be due to *in vivo* stress, caused by fluctuating

microenvironment conditions including temperature. When cells are exposed to temperatures significantly lower than 37, their internal structure begins to dismantle. Initially, the microtubules disassemble followed by the microfilaments, which results in a reduction of both mitosis and protein synthesis. Cells exposed to severe cold shock environment may arrest in a cell cycle growth stage such as G2 or undergo apoptosis (Fujita 1999).

3.2 TC32 ES Cells Exhibit Cellular Migration *In vivo*

From 0-48 hpi cells maintained close proximity near one another at the site of injection (yolk sac) (Figure 8). In most cases TC32 cells began to disseminate and travel away from one another within the anterior/head region of the embryos at 48 hpi. However, this initial observed movement was not attributed to active cell migration or metastasis because of natural mechanisms that occur within the fish, which could physically cause the passive spread of the cells. Over the first 7 days post fertilization the embryos gain the majority of the nutrients from their yolk sacs. Yolk sacs are consumed over this time frame until they have completely disappeared, which results in the formation of the ventral surface of the embryo. For this reason, I specifically confined my region of migration analysis to an anatomic area between the cloacae and the tip of the tail tissue. Attempts to analyze an area smaller than this might underestimate migration, as cells do not always travel to a distinct region of the tail tissue, rather they distribute through almost the entire tail. Cell migration of TC32 cells from the yolk sac to the distal tail regions of embryos was observed as early as 72 hpi. From 72 hpi onward, the cancer cell burden present within the XT recipient embryos became significantly high, which often resulted in mortality at 168 hpi. Moreover, given the remarkably high cell presence within the tail regions, it became difficult to effectively count

the number of cells for migratory evaluation. Migratory analysis was conducted at 24h intervals for 120 hpi. The presence of six or more cells in the tail regions was scored as a positive migratory event. Approximately 70% of all TC32 ctrl cell injected embryos displayed cell migration to the tail (Figure 10).

To demonstrate that this motility was indeed an active cellular process as that of cancer metastasis observed in human patients we used both TC32 cells fixed in 4% paraformaldehyde and TetraSpeckTM microspheres as controls (Figure 11). Both controls were injected using the same protocols executed for TC32 cell injection, at approximately 50-100 cells/microspheres per embryo and each displayed similar phenotypes at 24 hpi to that of TC32 cells. However, in contrast to the TC32 cells, neither of the experimental controls displayed cell migration to the tail at any time interval. In addition, *ex vivo* proliferation assays were performed on these controls to demonstrate that they were static objects with no ability to actively divide (Figure 12). These results suggest that TC32 ctrl cells are actively migrating to the tail tissue of embryos (Figure 13).

3.3 The Zebrafish XT Model Enables the Direct Observation of Key Steps in Metastasis

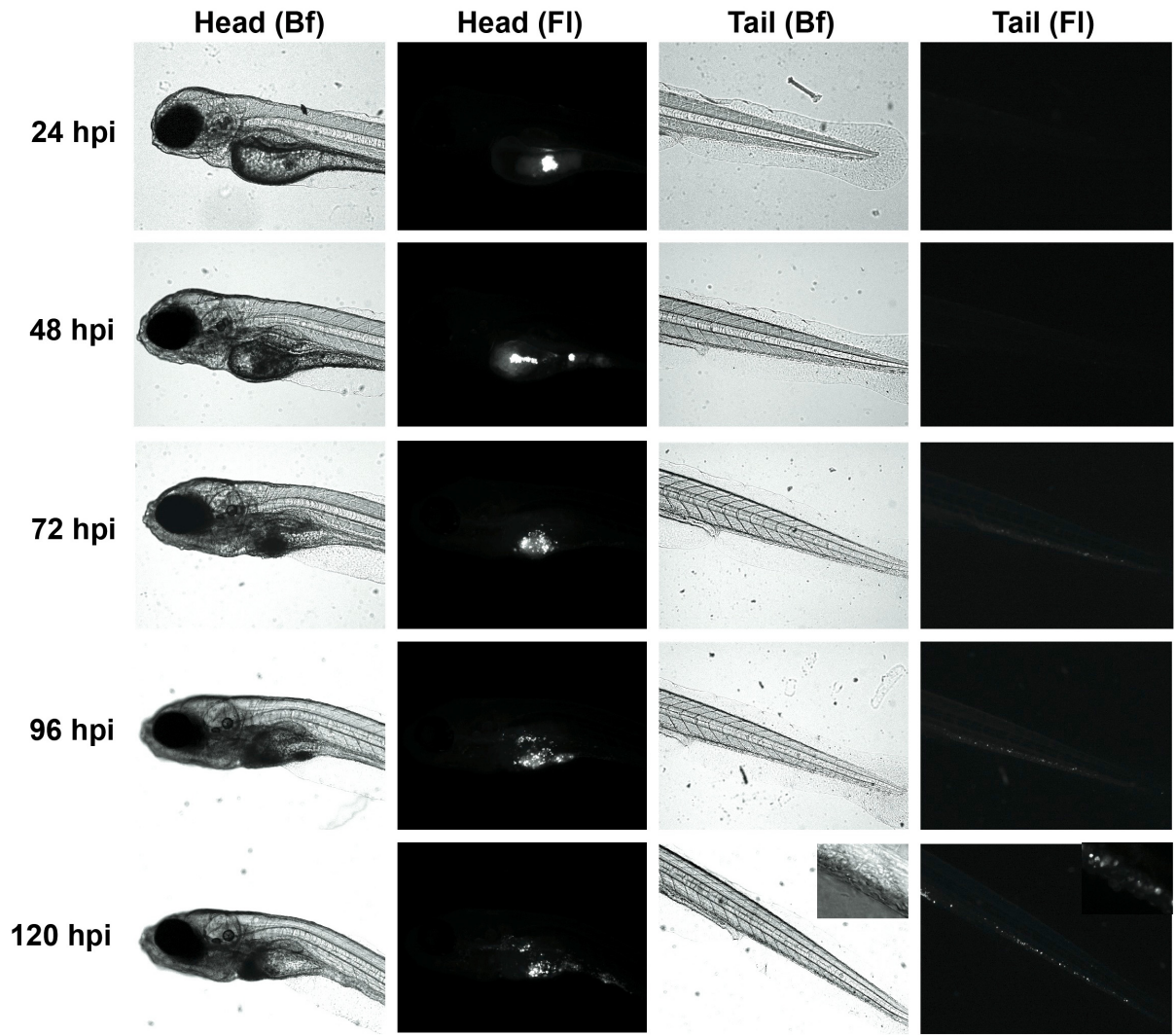
Upon the injection of TC32 ctrl cells we were able to observe and analyze what appeared to resemble some of the key steps associated with human cancer metastasis within the zebrafish XT, namely neoangiogenesis, ES cells in circulation and extravasation.

Using the *tg(filla:eGFP) casper* transgenic/mutant zebrafish lines we were able to study the direct interactions between our injected TC32 ctrl cells and the local vasculature. These zebrafish have green fluorescent blood vessels and possess the same whole body

transparency as the *casper* line. I was able to observe vasculature protrusions extending from zebrafish subintestinal blood vessels (Serbedzija, Flynn, and Willett 2000) towards the ES TC32 cell masses created from our injections (Figure 14). Using live cell microscopy and time lapse video capture techniques we were able to observe TC32 ctrl cells traveling directly through the established zebrafish vasculature from sites as far as the head region to the tail region. TC32 cells were observed traveling through the dorsal aorta, axial vein, and intersegmental vessels.

Given the optical advantages present in the *casper* embryos we were able to easily visualize the TC32 cells once they became embedded within tail tissue post-migration/metastasis (Figure 15a & 15b). The size of the TC32 ctrl cells (~12 μm) alone makes it fairly easy to detect them within tissue with fluorescence or by using differential interference contrast microscopy (DIC) – a contrast enhancing technique superior to brightfield microscopy. I have captured several images displaying potential TC32 cell interactions with the endothelial cell layers of blood vessels found in the tails of embryos. Cells were shown to stay stationary when in direct contact with the endothelial layer of the main axial vein vessel present in the embryo tail at one image capture (96 hpi) but by 120 hpi, these same cells were shown to have moved through the blood vessel wall and enter into neighbouring tail tissue (Figure 15c & 15d).

A



B

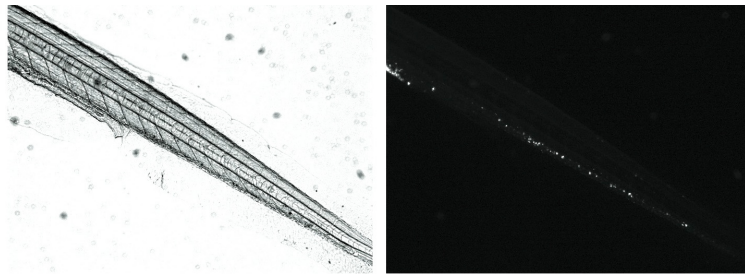


Figure 8. TC32 ctrl cells can be injected, survive, proliferate and migrate in the zebrafish xenotransplantation platform. TC32 ctrl cells, with wildtype YB-1 expression, were injected into the yolk sacs of 48 hpf *casper* embryos and were examined for *in vivo* cell behaviour within the zebrafish microenvironment over 120 hpi. These cells migrate to the tail as early as 72 hpi. Brightfield (Bf) images were taken of the head and the tail regions of the fish along with fluorescent (Fl) images of each region to reveal the injected TC32 ctrl cells (A). An enlarged panel of the 120 hpi tail images has been provided (B). Figure is displayed on prior page, 52. ctrl = TC32 cells injected with control shRNA. N= 10-15 embryos per experiment. Each single image frame corresponds to ~1.8 mm in length. hpi-hours post injection

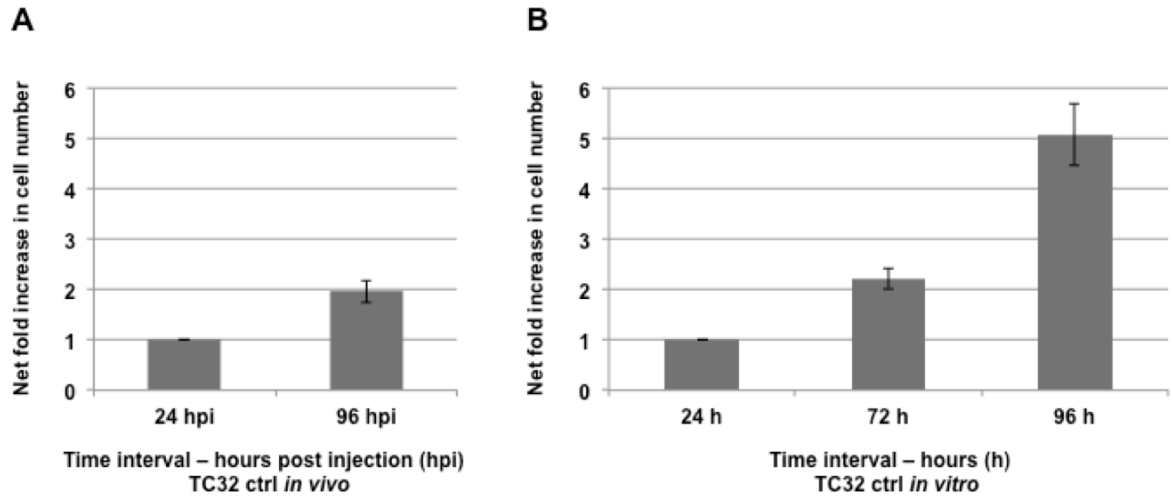


Figure 9. *In vivo* cell proliferation rate of TC32 ctrl cells is delayed compared to proliferation rates *in vitro*. *In vivo* cell proliferation rates were determined by enzymatically dissociating groups of 15-20 embryos at 24 hpi and 96 hpi and then analyzing the dissociated suspension using Image J software to detect the number of fluorescent ES cells labeled with Cm-DiI. *In vitro* rates were determined using a hemocytometer. Cell proliferation of TC32 ctrl cells *in vivo* doubled approximately at 96 hpi (A), comparable to the doubling that occurs at 72 hpi of these cells *in vitro* (B). At 96 hpi *in vitro* TC32 ctrl cells had nearly quintupled. N= 20 embryos for *in vivo* proliferation analysis. ctrl = TC32 cells injected with control shRNA. Error bars = \pm 1 standard deviation (SD). hpi- hours post injection

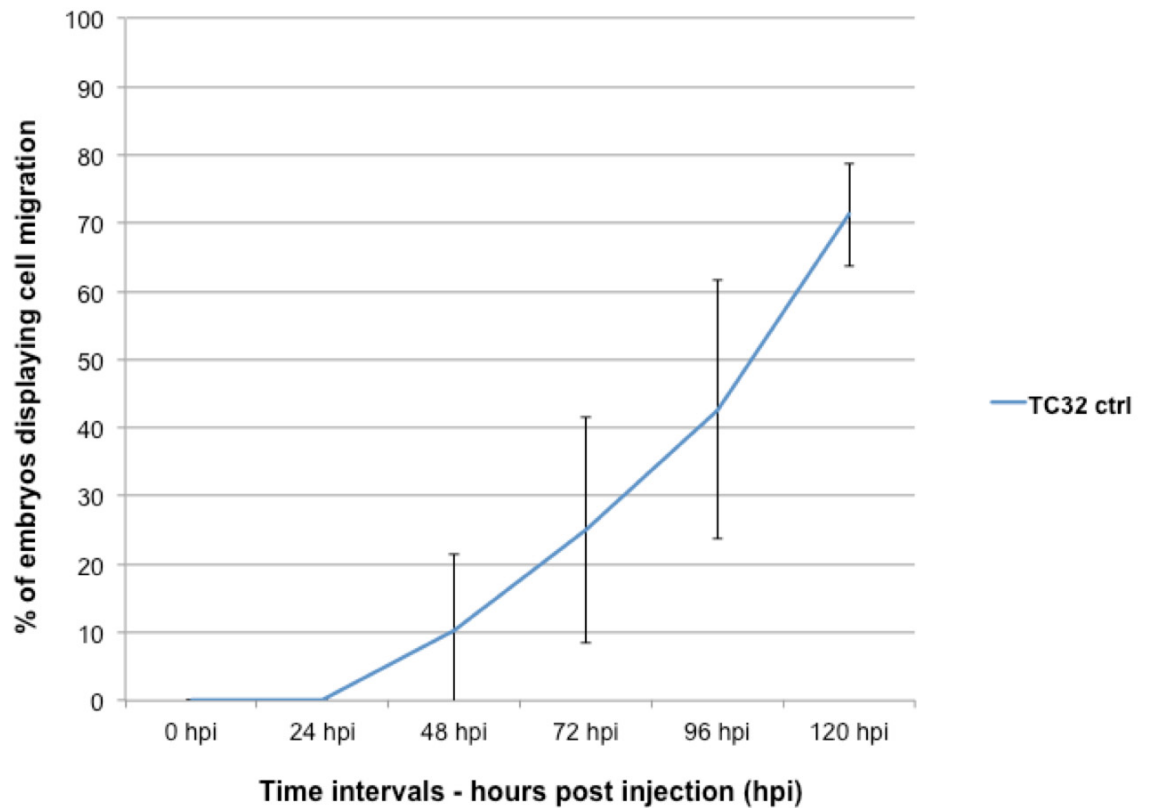


Figure 10. TC32 ctrl cells display cell migration in 70% of total injected embryos at 120 hpi. Groups of 30-40 embryos were observed over 120 hpi to examine the migratory capacity exercised by TC32 ctrl cells. Embryos were scored positively for a migratory phenotype if six or more cells were observed in the tail region of the embryo, precisely between the cloacae and the tip of the tail. By 120 hpi approximately 70% of all embryos, injected with TC32 ctrl cells, display cell migration to their tails. N= 70-100 embryos. ctrl = TC32 cells injected with control shRNA. Error bars = ± 1 standard deviation (SD). hpi- hours post injection

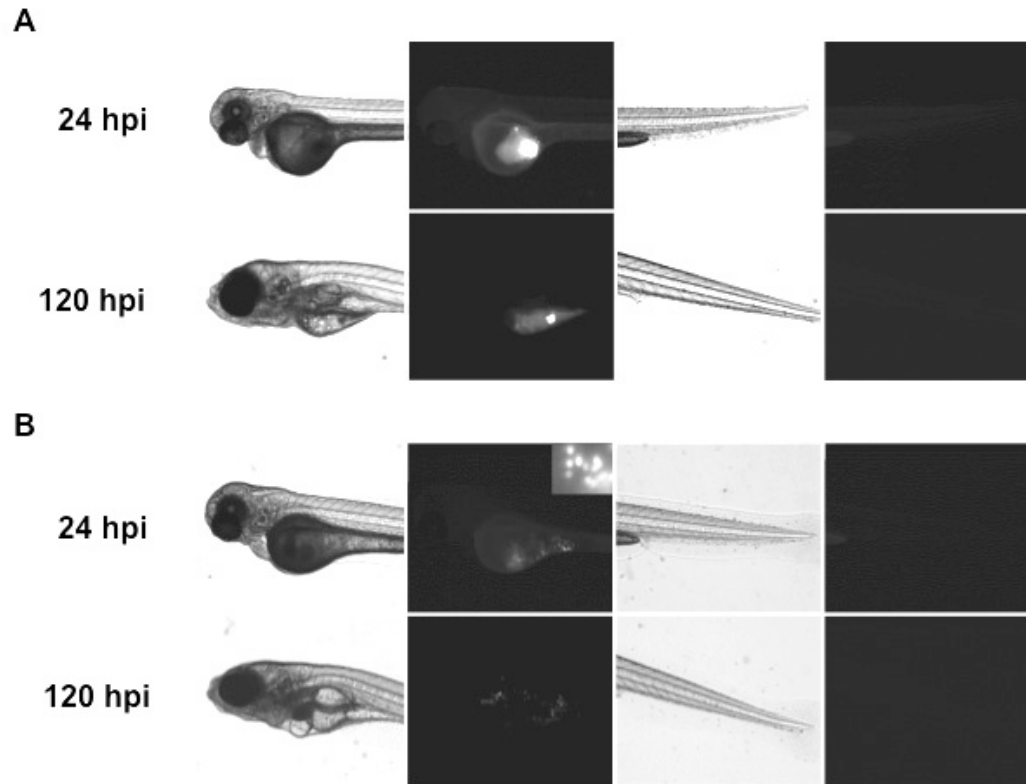


Figure 11. Live cell imaging of Fixed TC32 ctrl cell and TetraSpeck microsphere injected *casper* embryos reveal no observable cell migration. Approximately 50-100 fixed TC32 ctrl cells (A) or TetraSpeck (B) microspheres were injected using identical procedures performed for live TC32 cell injection. Both controls behave similarly to TC32 ctrl cells during 24 – 120 hpi within the anterior regions of the embryos. Fixed cells and spheres were seen moving about, from day to day, through the head region of the embryo throughout the majority of experiments, however, no cell or sphere migration to the tail regions is observed. Each single image frame corresponds to ~1.8 mm in length. N= 70-100 embryos per group. Migration experiments were completed in triplicate, hpi- hours post injection. ctrl = TC32 cells injected with control shRNA

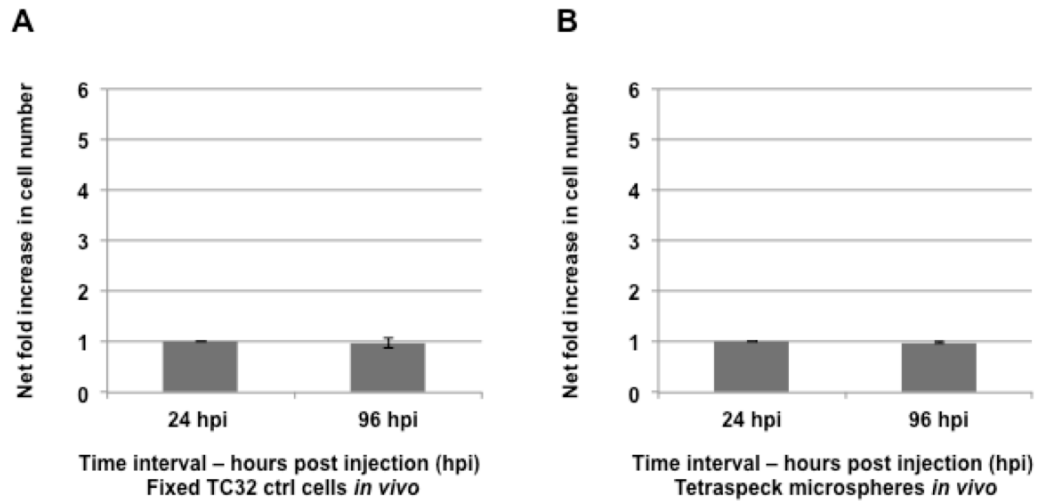


Figure 12. No significant differences in proliferation are observed for either fixed TC32 ctrl cells or TetraSpeck microspheres within 24 – 96 hpi. Cell proliferation rates were determined by enzymatically dissociating groups of 15-20 embryos at 24 hpi and 96 hpi and then analyzing the dissociated suspension using Image J software to detect the number of fluorescent fixed ES cells or microspheres. Neither fixed TC32 ctrl cells or TetraSpeck microspheres show any notably signs of proliferation from 24 – 96 hpi *in vivo*. N= 20 embryos proliferation analysis. Experiments were completed in triplicate. ctrl = TC32 cells injected with control shRNA. Error bars = ± 1 standard deviation (SD). hpi- hours post injection

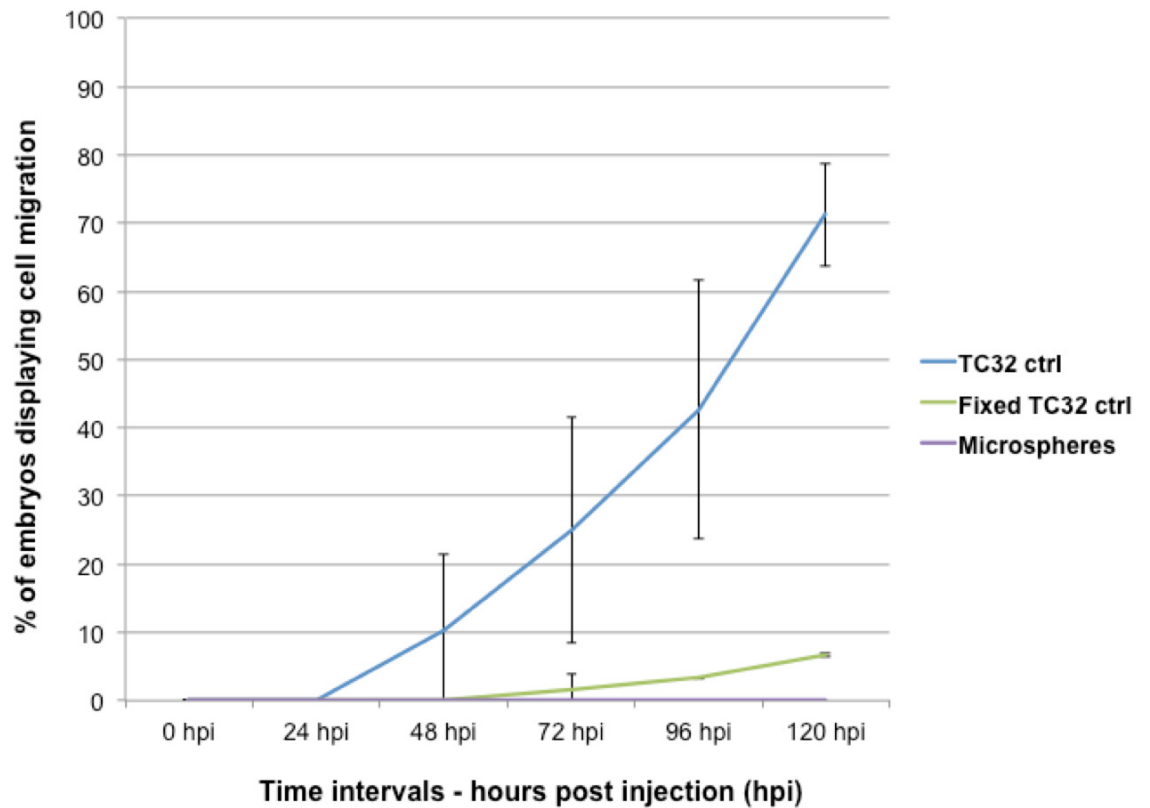


Figure 13. TC32 ctrl cells display active cell migration to the tail regions at 120 hpi in 70% of embryos. Neither of the experimental control groups, fixed TC32 ctrl cells or TetraSpeck microspheres, show any significant mobility within the injected embryos over 120 hpi. $p \leq 0.0001$ for TC32 ctrl migration vs. fixed TC32 cell migration at the 120 hpi time point. $N = 70-100$ embryos per injected cell group. Experiments were completed in triplicate. P value > 0.05 is deemed statistically significant. ctrl = TC32 cells injected with control shRNA. Error bars = ± 1 standard deviation (SD). hpi- hours post injection

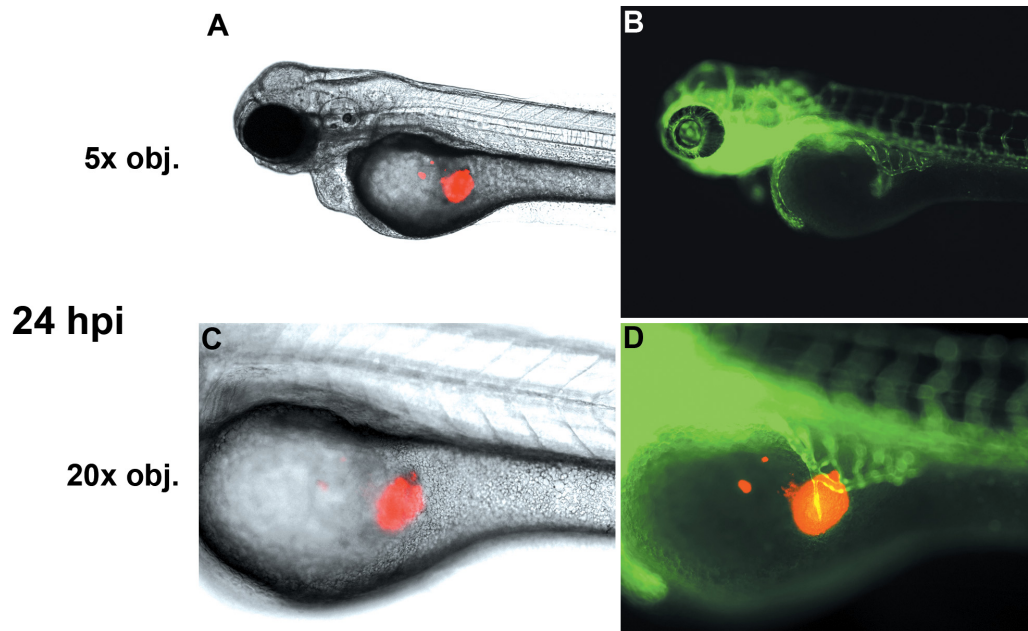


Figure 14. TC32 ctrl cells are observed interacting with host vasculature in *tg(fli1a:eGFP)* casper embryos . 5x objective (obj) Brightfield (A,C) and Fluorescent (B) merged (D) images display TC32 ctrl cell boli (red) and green fluorescent blood vessels (A). At 20x obj a protruding blood vessel was observed in close proximity to the injected TC32 cell bolus. 5x objective image frames correspond to ~1.8 mm in length. ctrl = TC32 cells injected with control shRNA. 20x objective frames represent ~ 0.8 mm. hpi- hours post injection, obj- microscope objective

3.4 TC32 YB-1 kd Cells Display Significantly Reduced Cellular Migration to the Tail

After examining the behaviour of TC32 cells with wildtype expression of YB-1, I wanted to assess the impact of YB-1 knockdown (kd) on TC32 cell behaviour, notably migration, *in vivo*. TC32 YB-1 kd cells were injected into 48 hpf *casper* embryos at 50-100 cells per embryo and then analyzed using live cell microscopy, the *ex vivo* proliferation assay and the migration assay to determine overall behaviour within the zebrafish tumour microenvironment.

TC32 YB-1 kd cells displayed similar behavior to TC32 ctrl cells at 24 hpi with the cell bolus localizing in the yolk sac and dissemination occurring in the anterior head region of embryos as cells proliferate (Figure 16a). Interestingly, TC32 YB-1 kd cells displayed reduced migratory capacity compared to TC32 ctrl cells, from 72 hpi onward (Figure 16b). The proliferation rate of TC32 YB-1 kd cells was 1.15 X greater than those of the TC32 ctrl cells. TC32 YB-1 kd cells more than doubled at 96 hpi while TC32 ctrl cells did not double until after 96 hpi. The *in vivo* proliferation of the TC32 YB-1 cells paralleled the rates observed *in vitro* (Figure 17). TC32 YB-1 kd cells doubled by 72 h *in vivo* and by 48 h *in vitro*. TC32 YB-1 kd cells displayed cell migration in 22% of injected embryos while TC32 ctrl cells displayed efficient cell migration in 70% of all injected embryos (Figure 18). Additionally, using IBM SPSS software, to calculate relative risk estimates, I determined that the likelihood of TC32 ctrl cells migrating to the tail regions was 3X more likely than for TC32 YB-1 kd cells (Appendix A).

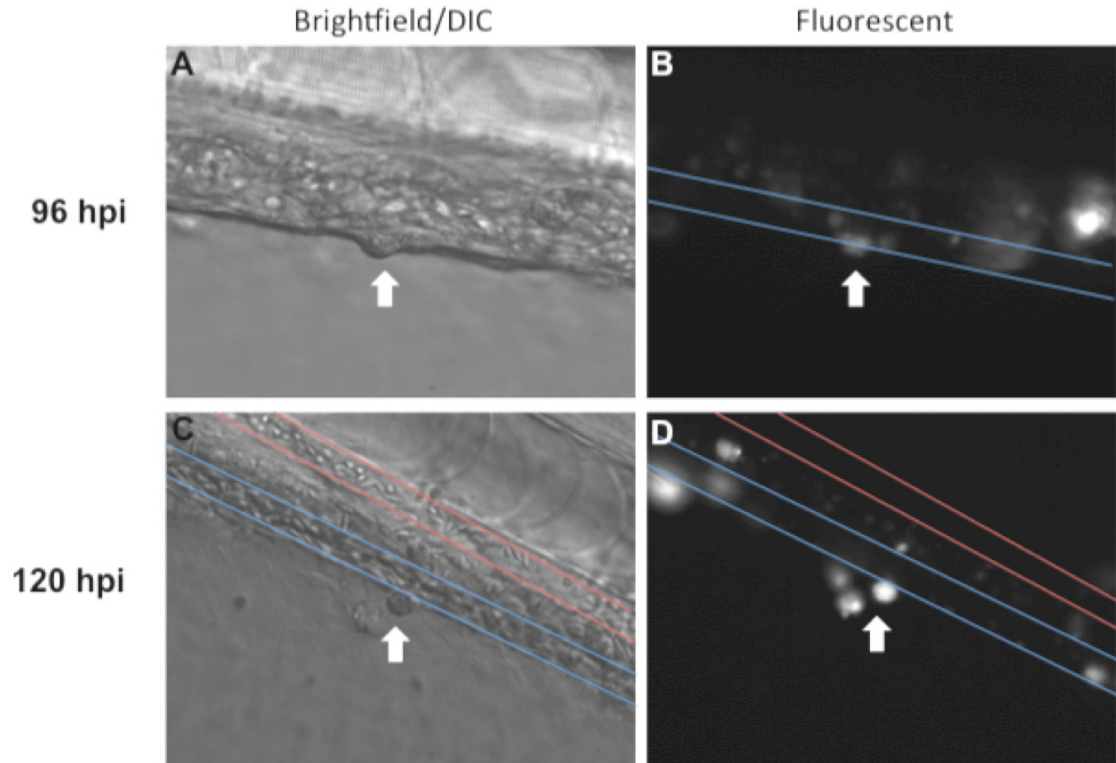
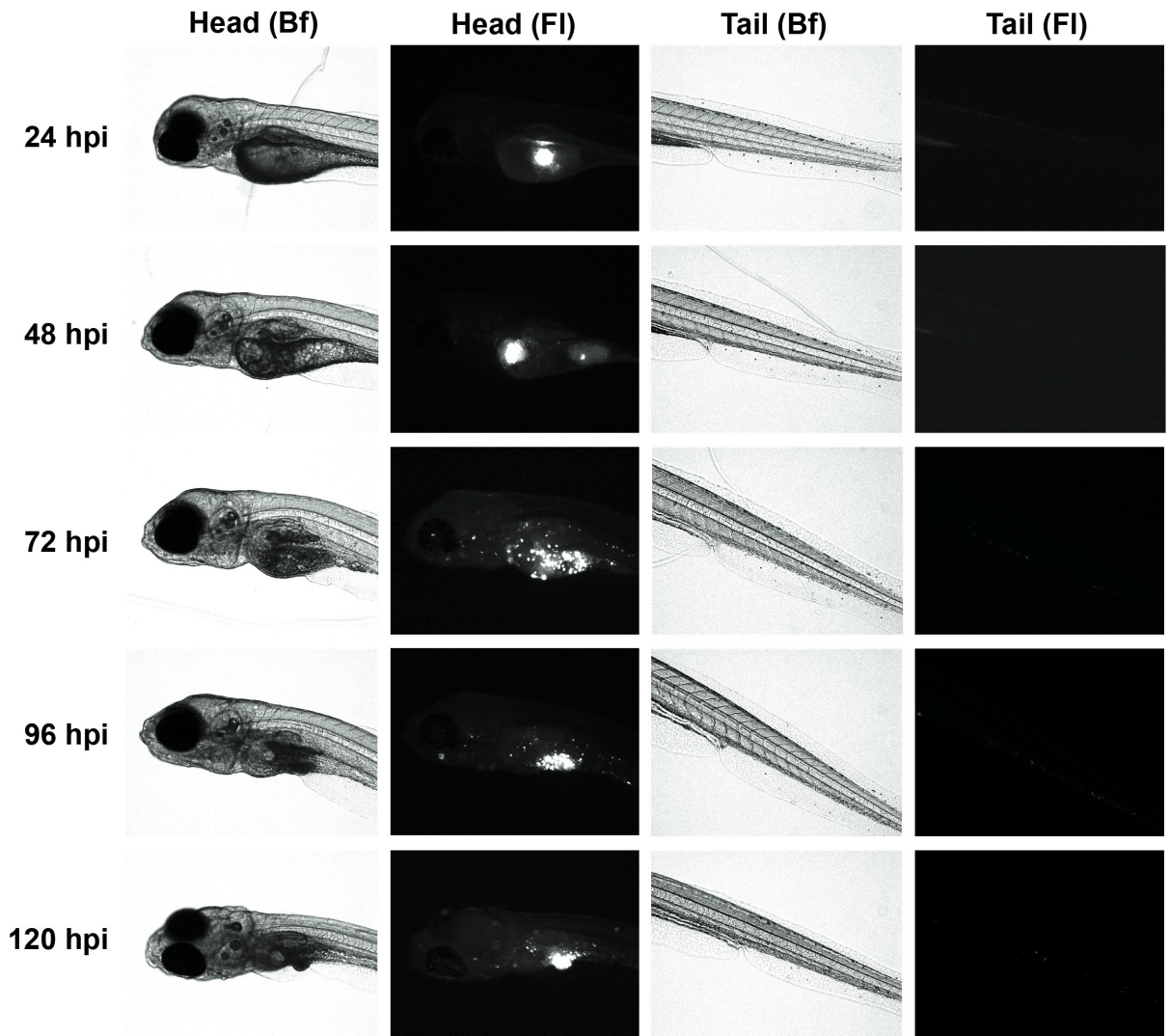


Figure 15. TC32 ctrl cells are capable of transitioning through the vasculature and extravasating into the tail tissue. TC32 ctrl were injected into 48 hpi *casper* embryos and their *in vivo* behaviour was observed through both anterior and posterior regional analysis using live cell microscopy. Embryo tail regions were imaged through differential interference contrast (DIC) microscopy (A,C) and fluorescent microscopy (B,D) to provide high magnification images of the intercellular events occurring in the tail. At 96 hpi TC32 ctrl cells were observed interacting with the blood vessel wall of the main vein found in the zebrafish tail. 24h later, at 120 hpi, this same group of cells was shown to have migrated into the neighbouring tail tissue of the presumptive fin. Each image frame corresponds to ~ 0.2 mm in length. ctrl = TC32 cells injected with control shRNA Arrows= cell group, red outline = dorsal aorta/artery and blue outline = axial vein. hpi- hours post injection.

A



B

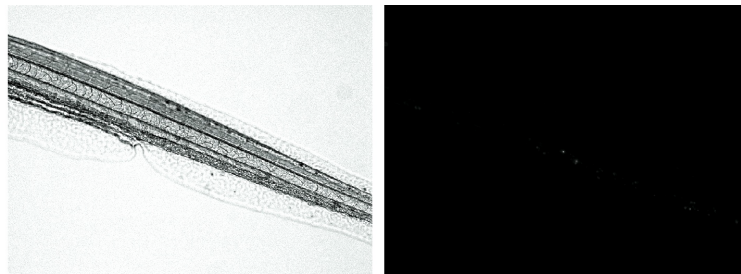


Figure 16. TC32 YB-1 kd cells display similar anterior cell migration but do not exhibit posterior cell migration to the tail region compared with TC32 ctrl cells. TC32 YB-1 kd, with significantly reduced YB-1 expression, were injected into 48 hpi *casper* embryos and examined for *in vivo* cell behaviour within the zebrafish microenvironment over 120 hpi. TC32 YB-1 infrequently migrate to the tail region. Brightfield (Bf) images were taken of both the head and the tail regions of the fish along with fluorescent (Fl) images of each region to reveal the injected TC32 YB-1 kd cells (A). An enlarged panel of the 120 hpi tail images has been provided (B). Figure is displayed on prior page, 62. N= 10-15 embryos per experiment. Each single image frame corresponds to ~1.8 mm in length. . kd = TC32 cells injected with YB-1 shRNA, hpi- hours post injection

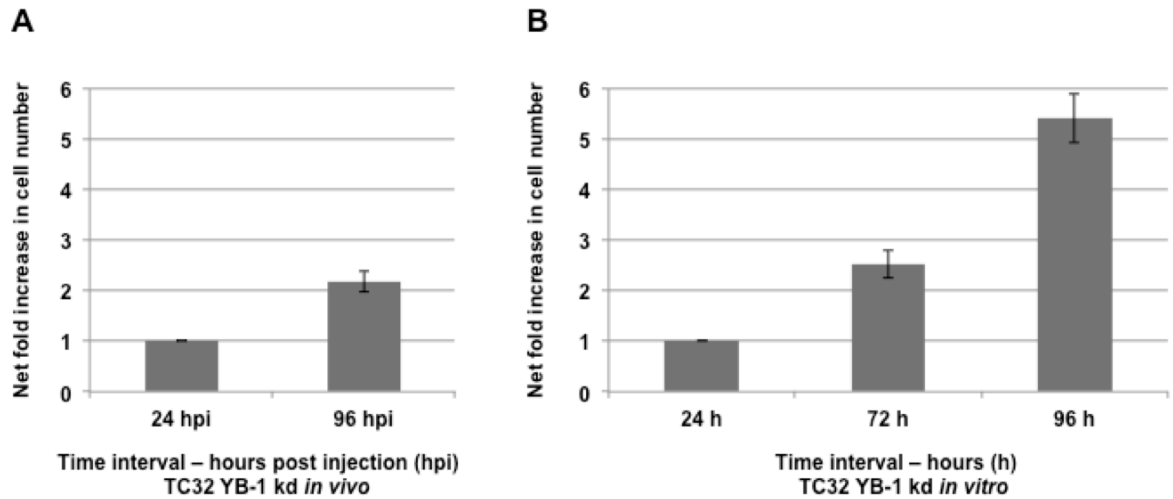


Figure 17. Cell proliferation of TC32 YB-1 cells *in vivo* is delayed compared to proliferation rates *in vitro*. *In vivo* cell proliferation rates were determined by enzymatically dissociating groups of 15-20 embryos at 24 hpi and 96 hpi and then analyzing the dissociated suspension using Image J software to detect the number of fluorescent ES cells labeled with Cm-DiI. *In vitro* rates were determined through hemocytometer counts. Cell proliferation of TC32 YB-1 kd cells *in vivo* doubled around 96 hpi (A), comparable to the doubling that occurs at 72 hpi of these cells *in vitro* (B). At 96 hpi *in vitro* TC32 YB-1 kd cells quintupled. N= 20 embryos for *in vivo* proliferation analysis. Experiments were completed in triplicate. Error bars = ± 1 standard deviation (SD). kd = TC32 cells injected with YB-1 shRNA, hpi- hours post injection

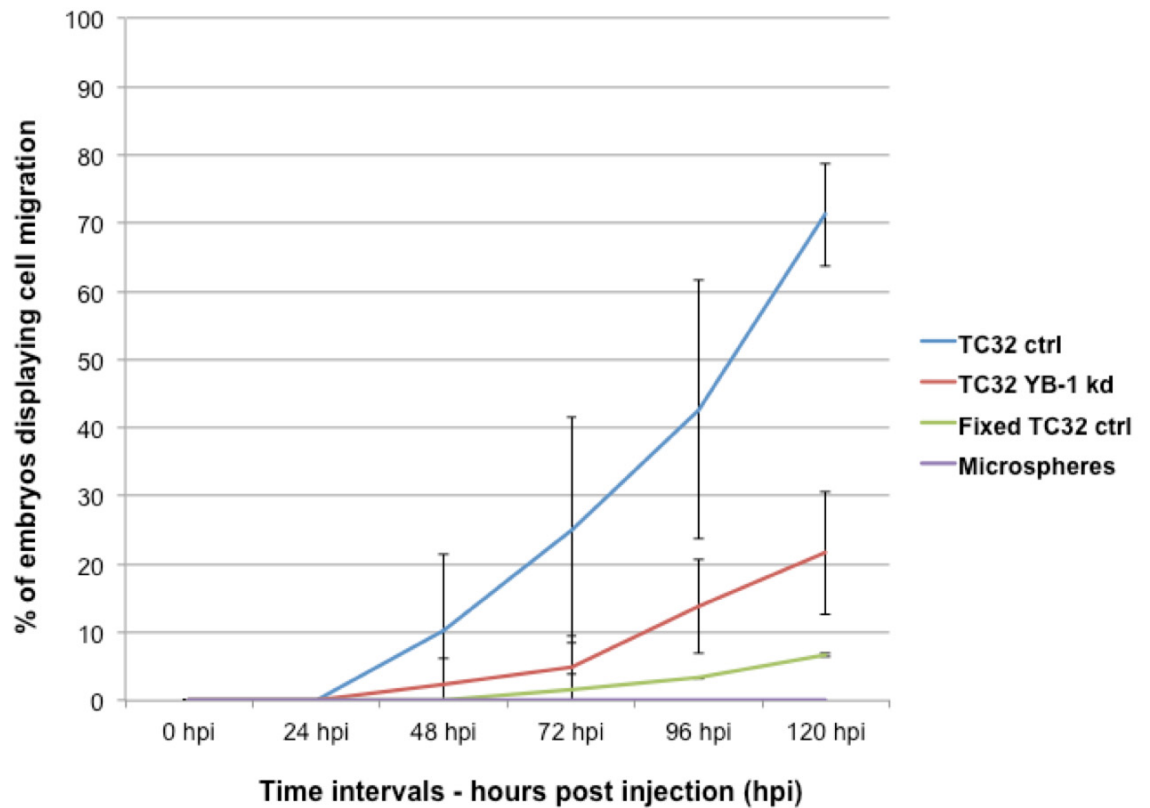


Figure 18. TC32 ctrl cells display increased cell migration to the tail region in contrast to TC32 YB-1 kd and controls. TC32 ctrl cells, TC32 YB-1 kd cells, fixed TC32 ctrl cells, or TetraSpeck microspheres were injected into the yolk sac of 48h *casper* embryos and monitored by fluorescent microscopy for 120 hpi. Quantification of migration was as described in Figure 7. At 120 hpi, TC32 ctrl cells migrate to the tail in approximately 70% of total injected embryos while in contrast the TC32 Yb-1 kd cells migrate to the tail in approximately 20% of embryos ($p \leq 0.0001$). No significant migration was observed for either fixed TC32 control cells or TetraSpeck microspheres. $N = 70-100$ embryos per injected cell group. Experiments were performed in triplicate. Error bars = + 1 standard deviation (SD) (ctrl = TC32 cells injected with control shRNA; kd = TC32 cells injected with YB-1 shRNA) hpi = hours post-injection

Chapter 4: Discussion

Though still emerging as a animal model for cancer research, the zebrafish has repeatedly proven to be useful and powerful in its application for furthering our knowledge on how many cancers progress and how we may be able to treat specific forms of cancer with targeted drug therapies (Beckman 2007; Berghmans et al. 2005; Etchin, Kanki, and a T. Look 2011; Feng et al. 2010; Flores et al. 2010; Lu et al. 2011; Mandrekar and Thakur 2009).

The goal of my research was to utilize the zebrafish as an *in vivo* xenotransplantation (XT) platform to study Ewing's sarcoma (ES) and investigate the role of one particular factor, Y-box binding protein 1, in the metastasis of ES.

4.1 The Zebrafish XT Platform can be Used to Study ES

Our zebrafish XT model has shown prior success in the determination of proliferation rate and drug response for human leukemia's (Corkery et al. 2011) and with the research presented in thesis, I have demonstrated the utility of the XT model for studying Ewing's sarcoma. I successfully introduced human ES cells into the zebrafish XT model. TC32 ES cells displayed active cell proliferation, dissemination and migration *in vivo* and were well tolerated overall by the zebrafish recipients, from 48-168 hours post fertilization (hpf). Moreover, I have shown how transgenic/mutant transparent *casper* zebrafish provide a unique tool to study the interactions that occur between tumour cells and surrounding microenvironment.

Given that localized ES patients have fairly optimistic overall survival, the focus of my research was to develop an *in vivo* model applicable for studying metastatic ES. I adapted

our current zebrafish XT model to study ES by determining the optimal number of cells that should be injected into recipient embryos; the best approaches for imaging and analyzing the ES cells *in vivo*; and the appropriate duration for monitoring of injected embryos to evaluate a migratory phenotype. I determined the optimal number of injected ES cells to be 50-100 cells per embryo for my experiments in order to enable cell migration without causing overwhelming cancer cell burden to the recipient embryos. The yolk sac was used as our primary site of injection due to ease of injection on account of its relative large size compared with other XT injection sites such as the axial vein and hindbrain. Moreover, the yolk sac is an easily accessible anatomic location within the mid body of embryos and due to the lack of major blood vessels at 48 hpf I could ensure I was not passively injecting cells into the vasculature, allowing for the natural examination of active cell migration characteristic of human cancer cells. The size of the yolk sac offers a high surface area to puncture with an injection needle, which is necessary when injecting into embryos with different orientations on the injection plate. Consequently, using the yolk sac as the injection site requires little realignment of the embryos during a round of injections to ensure successful positive injection.

Upon injection of TC32 ES cells, I determined it took approximately 72 hours post injection (hpi) before the injected cells began to migrate to the tail region of the recipient embryos. I observed a range of time intervals, from 48 – 96 hpi, for anterior dissemination of TC32 cells. I did not use the anterior region of the zebrafish embryo to quantify migration as this cell migration could have been coincidentally caused by natural biological processes inherent in the embryo rather than as a result of cell autonomous behaviour. In particular, I was concerned that the natural absorption of the yolk sac could have been passively forcing

the nearby cells to move about the anterior region of the embryos. As the yolk sac is consumed throughout the first 7-14 days of embryonic development, the ventral epidermal layer of the yolk sac propels upwards, destined to become what is the main ventral epidermis of the zebrafish. These speculations were confirmed specifically when we observed some anterior dissemination of fixed TC32 cells and TetraSpeck microspheres. The yolk sac may also play a role in the delay of *in vivo* cell proliferation compared to the levels observed *in vitro*. In addition, hormones or lipids, present as components of the yolk sac, as well as fluctuating levels in oxygen saturation might impact and potentially inhibit cell proliferation. By contrast, cells cultured *in vitro*, are not exposed to these varying microenvironmental conditions.

I employed the embryo tail region, from the cloacae to the tip of the tail, as the site in which to evaluate migration. I demonstrated that travel to this site required active migration only exhibited by injected living TC32 ES cells. To confirm that the motility I observed by the TC32 cells *in vivo* was indeed an active process, similar to metastasis in humans, I needed to conduct negative control experiments with materials that would not be expected possess any inherent active migratory capacity. Using my criteria for scoring cell migration to the tail region, fixed TC32 cells and the TetraSpeck microspheres displayed no significant migration within the zebrafish XT model. These results suggested that living TC32 cells were actively migrating throughout the zebrafish tumour-microenvironment, rather than passively. Following my results on TC32 cell migration, I began to analyze the specific behaviour of the cells *in vivo* before, during and after migration.

4.2 Zebrafish XT can be Used to Examine Specific Cancer Cell Behaviours

The ability of zebrafish XT to provide a tumour microenvironment and enable real-time examination of host-tumour interactions offers significant advantages to not only validate specific therapeutics and their targeted effects but also for uncovering unknown mechanisms involving all aspects of a tumour microenvironment. Using DIC microscopy, I specifically observed extravasation of TC32 cells in our zebrafish XT model. Given the size of an embryo we are able to analyze cellular interactions at the individual cell level at high resolution within almost any region of the body. I observed a group of TC32 cells at 96 hpi in close proximity to the endothelial cell wall of the axial vein present in embryo tail tissue. After 24h when I examined the same embryo I witnessed that the TC32 cell group has migrated out of the blood vessel lumen and into the tissue of the tail.

The zebrafish microenvironment provides the unique ability to examine, in real-time, the interactions between xenografted tumour cells and the host vasculature, extra cellular matrix, matrix-metalloproteinases and specific immune cells. Extracellular matrix (ECM) remodeling is a crucial process in animal embryonic development, wound healing and the growth and metastasis of tumours (Hartenstein et al. 2006; Overall and Kleinfeld 2006). The primary effectors of ECM remodeling are matrix-metalloproteinases (MMPs) and their function in the degradation of the ECM is required for endothelial cell migration and subsequent tumour angiogenesis (McCawley and Matrisian 2000). Wyatt et al have developed two novel zebrafish assays, differential *in vivo* zymography and activity-based protease profiling, capable of analyzing and detecting active MMPs *in vivo* (Wyatt et al. 2009).

A transgenic zebrafish line, *tg(mpo:eGFP)* with GFP expression under the neutrophil-

specific myeloperoxidase (mpx) promotor, has been developed to offer the direct analysis of zebrafish neutrophils *in vivo* (Renshaw et al. 2006). Additionally, transgenic zebrafish with GFP expression under macrophage expressed gene 1 (*mpeg1*), *tg(mpeg1:eGFP)* are available to examine the behaviour of macrophages *in vivo* (Ellett et al. 2011). We are interested in employing these lines of zebrafish for our own ES studies. Given our distinct differential migratory phenotypes within our ES XT platform, TC32 ctrl cells with high migratory capacity and both fixed TC32 ctrl cells and TetraSpeck microspheres with low migratory capacity, we could analyze the interactions between host immune cells and tumour cells. It would be interesting to see if a difference in immune response is observed between our high migrating and low migrating cell/sphere groups. Perhaps the cell groups that display less migration to the tail regions are eliciting a more significant immune response from the zebrafish, thus restricting the cell population to stay localized anteriorly.

Recently He et al., (2012) showed that by blocking VEGF receptors in a zebrafish xenograft model, tumour vascularization could be reduced. Interestingly, this inhibition resulted in the enhanced migration and recruitment of neutrophils to the primary locations of tumour cells and promoted their migration even without the presence of blood vessels (He et al. 2012). This example demonstrates the importance of the microenvironment and how it influences cancer behaviour and concurrent progress. The availability of these transgenic lines offers an effective means to observe the interactions of specific innate immune cells with tumour cells within the zebrafish microenvironment.

4.3 Using the Zebrafish XT Platform to Model Human Metastatic Events

In my migration studies, I have consistently observed cell migration to the tail region of embryos from the initial injection site, the yolk sac. I have confirmed that fixed TC32 cells, as well as TetraSpeck microspheres do not migrate to the tail regions. These results are based on the migration assay that I have developed, which attributes six or more observed cells in a XT recipient embryo tail as positive cell migration. We are currently revising this migration assay, to function in partnership with Image J software, to provide a more unbiased means to evaluate cell migration and additionally quantify the approximate number of migratory cells that travel to the tail tissue.

It appears as though the migration of TC32 cells, along with the extravasation events that I have observed, may represent metastasis within the zebrafish. However, these results remain inconclusive until we can visualize all of the specific steps in the metastatic cascade and the associated microenvironment interactions, such as inflammation and tissue remodeling. Histological sectioning of zebrafish, fixed at the time of cellular migration, would reveal the components of the microenvironment during these events, such as the presence of immune cells, and also the location within the embryo of where the ES cells have embedded. The injection of non-malignant cells such as human fibroblasts, which would not be expected to exhibit the same migratory capacity of the malignant TC32 cells, could also be injected into our XT platform as an additional negative control. Moreover, we could investigate the behaviour of local zebrafish innate immune cells through the use of immune cell specific zebrafish transgenic lines, such as *tg(mpeg1:eGFP)* (Ellett et al. 2011) and *tg(mpo:eGFP)* (Renshaw et al. 2006). Immune cells are known to play roles in both

preventing and promoting cancer formation (Dalglish 2005; Kees and Egeblad 2011; Whiteside 2006; Yu and Rak 2003). We are currently working toward developing a *tg(mpeg1:eGFP) casper* zebrafish line, to allow both transparency of the entire zebrafish and surveillance of fluorescent macrophages for use in sarcoma xenograft studies.

4.4 Studying Early Metastatic Events (Neoangiogenesis) in the Zebrafish XT Platform

Cancer metastasis is a complex cascade involving several notable key steps in successful progression. The ability to study each of the steps individually has tremendous promise to uncover aspects of metastasis and to allow the development of new therapies for invasive disease that act at a specific stage of metastasis.

During cancer progression, tumour growth requires a sufficient supply of oxygen through adequate access to a blood supply. Angiogenesis, the formation of new blood vessels from the existing parental vasculature, has been described as one of the hallmarks of cancer (Gupta and Massagué 2006; Chaffer and Weinberg 2011; Hanahan and Weinberg 2011). Neovascularization promotes tumour survival and subsequent dissemination and metastasis. The inhibition of angiogenesis has been applied as a potential treatment to inhibit tumour expansion and overall cancer progression (Heine et al. 2011; Quan and Choong 2006; Quesada, Muñoz-Chápuli, and Medina 2006). Vascularization plays a major role in the growth and progression of ES (Bolontrade, R. Zhou, and Kleinerman 2002).

Several researchers have recently presented elegant work using zebrafish embryos expressing GFP, *tg(fli1a:eGFP)*, to study angiogenic interactions with and recruitment to *in vivo* tumour cell masses (Nicoli and Presta 2007; Serbedzija, Flynn, and Willett 2000). *Fli1a* or Friend of leukemia integration 1a is an important transcription in the development of

blood vessels. Fetal liver kinase 1 (*Flk1*) is a vascular endothelial growth factor receptor, which when driving GFP expression, produces zebrafish embryos with green fluorescent endothelial cells (Becker et al. 2001). One group visualized the process of tumour neovascularization in high-resolution using *tg(flkl:eGFP)*. Evidence of very early angiogenic sprouting from host vessels into and around nearby injected tumour cells was demonstrated (C. Zhao et al. 2011). Ewing's sarcoma has been showed to utilize vasculogenesis for tumour expansion and subsequent metastasis through the increased production of VEGF (Bolontrade, R. Zhou, and Kleinerman 2002; Kumar et al. 2012).

In my study, one of the earliest observations I made, using *tg(fli1a:eGFP)* zebrafish embryos, was similar angiogenic recruitment to the site of tumour cell injection at 24-48 hpi. Using the *tg(fli1a:eGFP)* *casper* embryos, I observed direct vasculature interaction with TC32 cell masses in the yolk sacs of injected embryos. Subintestinal (SI) blood vessels, found just above the yolk sac, rather than the ducts of Cuvier, located in the anterior yolk sac near the heart, appeared to protrude ventrally toward the cell mass. I observed one primary blood vessel in close proximity to the bolus of injected TC32 cells. These blood vessel sprouts appeared relatively thick near the origin of the SI blood vessels but were more tapered and narrower close to the cell bolus. These observations were made on numerous experimental occasions and we hope to further investigate these interactions. A primary tumour needs a sufficient blood supply to adequately grow, disseminate and for most cases, to metastasize (Yokota 2000; Zetter 1998). These results could be interpreted as some of first observable steps in the metastatic cascade.

4.4.1 Targeting Angiogenesis in Ewing's Sarcoma

VEGF is one of the most potent stimulators of blood vessel production and expansion (Kaya et al. 2009). Cancer cells have the ability to express high levels of VEGF, which results in the recruitment of host blood vessels that form chaotic microvasculature around a developing tumour (Judah Folkman 2006; Douglas Hanahan, R. A. Weinberg, and Francisco 2000). Many targeted anti-angiogenic cancer drugs currently being developed and researched, are antagonistic against VEGF and block its production or inhibit its function by inactivation. The prototypic anti-angiogenic drug is bevacizumab (Avastin®), a monoclonal antibody that inhibits VEGF signaling, which has been approved for use in several malignancies in combination with traditional chemo- and radiotherapy (Andre et al. 2012; Yang et al. 2003; Crane et al. 2006). Avastin® has been shown to inhibit tumour angiogenesis in pre-clinical models of rhabdomyosarcoma, Wilm's tumour and neuroblastoma (Gerber et al. 2000; Rowe and Stolar 2000; Segerström et al. 2006).

It would be interesting to investigate the affects of some of these anti-angiogenic drugs in our zebrafish XT platform for ES to determine if they inhibit the overall survival or metastasis of the disease. These studies could employ the *tg(fli1a:eGFP)* zebrafish line, with injected ES cells. However, live cell imaging techniques would need to be enhanced to enable high resolution capture of the microscopic angiogenic effects such as micro-vessel sprouting and formation around the injected tumour cell masses in real-time. Two-photon confocal laser scanning microscopy could be used for observations of these studies given its ability to analyze an increased degree of tissue depth, produce 3-D real-time projections and Z stacks of whole embryo bodies (Carvalho and Heisenberg 2009). Additional protocols for live cell imaging of zebrafish embryos, for extended periods of time (2-8 h), could also be

developed and/or adopted to enable real-time video capture of the tumour microenvironmental events occurring between the host vasculature and the injected tumour cells.

We are currently pursuing the effects of Avastin® and other anti-angiogenic agents on ES cell progression in our zebrafish XT platform. I have conducted toxicity curves and have determined the optimal dose for zebrafish studies to be 0.25- 0.5 mg/ml. This dose represents the IC₅₀ value for Avastin® *in vivo*. Next, we will incubate ES cell injected embryos with this optimal dose of Avastin® and observe its effects on *in vivo* behaviour of the cells and the local vasculature. By inhibiting the action of available VEGF, Avastin® may concurrently reduce overall TC32 cell migration.

4.5 YB-1 Promotes Migration and/or Metastasis of ES in the Zebrafish XT Model

YB-1 is highly upregulated in a variety of human cancers including sarcomas (Matsumoto and Bay 2005; Oda et al., 1998). However normal tissues, from which these cancers originate, express relatively low levels of YB-1, providing strong evidence for its involvement in establishing and/or promoting cancer (Eliseeva et al. 2011). While YB-1 has been extensively examined in several human malignancies, studies investigating the role of YB-1 in childhood sarcomas have only been recently emerging. I used TC32 ES cells with ctrl shRNA and TC32 ES cells with YB-1 shRNA knockdown to examine the effects of YB-1 on ES migration in the zebrafish XT platform.

Compared to TC32 ctrl cells, with wildtype expression of YB-1, the TC32 YB-1 kd cells showed dramatically decreased cell migration within the injected embryos. While TC32 ctrl cells could successfully migrate in 70% of injected embryos, TC32 YB-1 kd cells

displayed migration in less than 25% of embryos. These observations correlated with *in vitro* studies, conducted by the Sorensen Laboratory, that suggest YB-1 promotes/confers metastatic capacity in ES cells and when its expression is reduced, mobility is concurrently affected. The Sorensen Laboratory has also observed similar migratory phenotypes of TC32 YB-1 using a mouse renal subcapsule model of ES (Amal El-Naggar & Poul Sorensen, personal communication). The number of mouse pulmonary nodules produced by transplantation of TC32 YB-1 kd cells were significantly reduced compared to what was observed for TC32 ctrl cells. These results highlight YB-1 as a potential key protein to uncovering additional new downstream targets against ES metastasis.

The specific mechanism by which YB-1 promotes metastatic capacity in ES remains elusive. It would be useful to further analyze the contribution of YB-1 to cell migration in other ES cell lines such as TC71, FPBH, SAL-2 and/or the CHLA9 (cells from primary tumour source that have wildtype expression of YB-1) and CHLA10 (cells from metastatic tumour source that have increased YB-1 expression), to confirm studies in the Sorensen laboratory, implicating YB-1 has similar roles in metastasis for a variety of ES cell lines. In addition, other childhood sarcoma cell lines including osteosarcoma and rhabdomyosarcoma, could be examined to determine if the same impact on migration occurs in these malignancies.

4.6 YB-1 Upregulation may cause Increased Angiogenic Recruitment to Promote Metastasis

YB-1 has been shown to promote EMT in breast cancer cells. However, given the speculated mesenchymal origin of ES it is unlikely that these cells would need further

transformation from an already apparent mesenchymal morphology. ES utilizes VEGF signaling to recruit host blood vessels for both adequate nutrient supplies and for effective metastasis. YB-1 may promote VEGF, which would explain why YB-1 is upregulated in metastasizing but not stationary tumour cells such as those of a primary tumour. It is also possible that high levels of VEGF could be associated with a primary tumours quest for a blood supply to sustain its own growth, rather than solely for means of migration. CHLA9 and CHLA10 cells, derived from the same ES patient, express these phenotypes of differential levels of YB-1 expression. CHLA9 cells were isolated from a primary tumour, and express low levels of YB-1, while CHLA10 cells, obtained from a metastatic cell population, have increased expression of YB-1 (Poul Sorensen, personal communication 2011). If YB-1 kd cells were unable to produce sufficient levels of VEGF or other angiogenic factors including fibroblast growth factor, it could be speculated that they would be less likely to metastasize due to the lack of available blood vessels for migration.

The zebrafish ES XT platform is well qualified to investigate the relative effects of anti-angiogenic inhibitors on ES cell migration. As mentioned above, *tg(fli1a:eGFP) casper* embryos could be used to directly visualize the interactions occurring between tumour cells and the host vasculature in the presence of an angiogenic inhibitor.

To determine if YB-1 is promoting ES metastatic capacity by upregulating the expression of vascular endothelial growth factor (VEGF), we would inject both groups of TC32 cell lines, ctrl and YB-1 kd, into the *tg(fli1a:eGFP) casper* embryos and examine how the tumour cell interactions with the host vasculature compare between the two TC32 cell lines. I would anticipate that given the reduced events of cellular migration, potentially caused due to a lack of angiogenic recruitment, there would be less angiogenic activity in the

TC32 YB-1 kd xenografts.

4.6.1 Determining the Downstream Factors of YB-1 that Promote ES Metastasis

Since YB-1 mediates increases in invasiveness and metastatic capacity in breast cancer cells through translational up-regulation of Snail and Twist (Evdokimova et al. 2009), it was speculated that a similar mechanism could explain YB-1 effects on sarcoma cell invasiveness. However, neither *Snail* nor *Twist* was prominently expressed in ES and was not affected by YB-1 expression levels. Of the other candidate EMT-related proteins that were shown to be upregulated in the breast cancer YB-1 studies hypoxia inducible factor 1 alpha (HIF1 α), was consistently induced in YB-1 expressing sarcoma cell lines, and dramatically reduced by YB-1 kd in the same cells. HIF1 α is a key transcription factor that regulates glycolysis and angiogenesis. In times of oxygen deprivation, tumour cells will increase the cellular abundance of HIFs to activate genes that promote angiogenesis, anaerobic metabolism and cell survival. The Sorensen Laboratory has shown that HIF1 α is consistently expressed in high YB-1 expressing sarcoma cell lines including CHLA10 ES cells. Moreover, HIF1 α expression is dramatically reduced in YB-1 kd cells (Poul Sorensen, personal communication 2012). Non-malignant or healthy cells found in the human body in microenvironments with sufficient or rich oxygen concentrations, employ the proteasome to degrade HIF1 α , resulting in minimal expression (Giatromanolaki et al. 2010). However, under hypoxic conditions this degradation fails to occur and HIF1 α accumulates within the cytoplasm of oxygen-deprived cells. This abundance can lead to increased cell survival, drug resistance and invasiveness, specifically in childhood sarcomas including ES (Kilic et al. 2007). Given that VEGF is a major downstream target gene of HIF1 α , it is possible that this

pathway plays a role in conferring enhanced migratory capacity in ES, due to increased tumour cell interaction with host vasculature from increased VEGF. Moreover, because increased HIF1 α expression is also associated with increased YB-1 expression, YB-1 could be regulating HIF1 α and by default, VEGF activity.

Using our *in vivo* ES XT platform, we could transplant ES cells, with high, wildtype or low expression of HIF1 α , such as CHLA ES lines, and examine the interactions with the host vasculature. If YB-1 does regulate levels of HIF1 α and HIF1 α promotes VEGF expression, we would expect to see increased angiogenesis in high expressing YB-1 and HIF1 α xenotransplanted cells. These experiments could be followed by the XT of ES cells, with naturally high levels of YB-1 and associated HIF1 α such as the CHAL10 line that have been transfected with shRNA targeted against HIF1 α . If no difference in migration is observed in ES cells with shRNA for HIF1 α , it may suggest that YB-1 is regulating metastatic capacity by other means. Subsequently we could overexpress HIF1 α levels in YB-1 kd cells and determine whether or not migratory capacity is reestablished to the level of ctrl cell equivalents. These studies would further determine if ES cell migration might be regulated, at least in part by increased HIF1 α expression and subsequent VEGF production.

In collaboration with the Sorensen Laboratory, we could substantiate any observed migratory effects of ES cells in the zebrafish XT platform, with differential HIF1 α , using the mouse renal subcapsule XT model. In the renal subcapsule model, xenograft cell blocks of luciferase-labeled ES cells are transplanted under the surface of the kidney. It has been shown that TC71 and TC32 cell blocks can proliferate within the kidney subcapsule cavity and metastasize to the lungs. We will employ both the zebrafish ES XT model and the

mouse renal subcapsule XT model to bridge both *in vitro* and *in vivo* studies, to determine and confirm the potential connection between YB-1, HIF1 α and VEGF, and the role these factors play in the metastasis of ES.

4.7 Advantages and Limitations to the Zebrafish XT Platform

The zebrafish XT platform offers exciting opportunities to study real-time human cancer cell behaviours *in vivo* that cannot be examined in traditional animal models including key steps in metastasis such as neoangiogenesis, intravasation and extravasation. The zebrafish XT model can be used alongside current cancer models for the continued study of human cancers. Zebrafish have specific utility to elucidate molecular mechanisms underlying oncogenesis by virtue of ease of genetic manipulations; observations of invasive cellular phenotypes, due to embryonic transparency and unique imaging; and as a relatively high-throughput cost-effective first pass *in vivo* platform to evaluate drug responses to prospective anti-cancer agents.

However, there remain several biological limitations when using zebrafish as a host for human cancers. Though many of the cancer genes and pathways observed in humans are highly conserved (Feitsma and Cuppen 2008; Payne and T. Look 2009; Stoletov and Klemke 2008), the zebrafish is a different species in which we are introducing foreign human cancer cells. For XT studies, zebrafish embryos are exceptional recipients for tumour cell injection because they lack complete full adaptive immunocompetence, with adaptive immune cells only becoming functional at 4-6 weeks post fertilization (wpf) (Lam et al. 2004). The zebrafish does develop many of the innate immune cells (macrophages, neutrophils, mast cells) observed in humans during early embryonic develop, enabling the analysis of innate

immune cell activity *in vivo* (Traver et al. 2003; Dobson et al. 2008, Da'as et al. 2011).

Specifically concerning metastasis, the zebrafish does not offer a long lifespan to study tumour cell dormancy, which can be associated with human metastatic disease. Human cancer cell-related dormancy is believed to exist for many years before a group of migrated cells may become detectable through typical diagnostic scanning. The lifespan of the zebrafish is two- five years. Our research team maintains zebrafish for two years, due to animal care protocols and procedures including risk of injection and spontaneous tumour formation in older fish. Therefore we may not be able to visualize secondary tumour formation as ES cells may present in a dormant state following migration. To overcome this lifespan specific limitation, one option would include performing serial transplantation experiments for future characterization of a migrating/migrated cell population (Taylor and Zon 2009). Cell populations that have migrated to the tail regions of embryos could be isolated and injected into new/younger zebrafish embryo recipients, which would facilitate further live-cell analysis. One difficulty that may arise during serial transplantation experiments could be the effective isolation of the tail region specific cell populations. The tail region of the zebrafish is fairly small and would need to be separated from the anterior/head region, which contains cells that have likely not migrated. Embryo size alone, approximately 3.5 mm in length from 48 – 168 hpf, may impede the ability to precisely separate the embryo head region from the tail regions.

Using Cm-DiI cell labeling I have been able to follow and visualize ES cells *in vivo*, observing how they behave and interact with the zebrafish microenvironment. However, a limitation of using Cm-DiI to label tumour cells for XT is its weakening fluorescence that occurs sequentially, with each cellular division. As the labeled cells divide, there is a 50%

reduction of Cm-DiI in each daughter cell resulting in 50% less fluorescence. We do not observe a dramatic loss in fluorescence during the first 7 dpi of our XT analysis, however, to enable longer observation intervals, we would like use more permanent means of labeling cells, such as incorporating GFP or mCherry. CM-DiI has been shown to allow viable cell tracking in mice for up to three to five months, however these experiments were analyzing lymphocytes, which would not have the proliferation capacity of cancer cells (Andrade et al. 1996). In addition, it is possible that the decreasing fluorescence of actively dividing cells may confound the determination of cell proliferation and cell migration. In future studies, cell proliferation should be measured at intervals later than 96 hpi to determine if the injected cancer cells retain optimal fluorescence necessary for cell detection. Cells that are permanently labeled with GFP or mCherry fluorescent constructs could be used in parallel with Cm-DiI labeled cells to determine if proliferation rates are similar between each group. If GFP labeled cells displayed an increased proliferation compared to Cm-DiI labeled cells, it could be a result of significant reduction in dye retention by the Cm-DiI cells.

4.8 Conclusion

In summary, this research has demonstrated some of the attributes that make the zebrafish a novel and versatile model for studying human cancers. I have developed a zebrafish XT platform for studying Ewing's sarcoma in real-time with specific emphasis on cell migration. I have created a migratory assay capable of quantifying cell migration from the site of injection, the yolk sac, to the tail region of the zebrafish embryo and have shown that YB-1 appears to play a role in ES cellular migration *in vivo*. I believe in the future that this XT model could be easily applied to drug discovery and drug evaluation studies. The ability to determine cell proliferation rates, detect and quantify cell migration, and analysis *in vivo* cancer cell behaviour, occurring in real-time, within a tumour microenvironment, positions this animal model as a powerful tool for the unbiased screening of anti-cancer agents that may inhibit the progression of ES.

References

- Akhtar, Kamal, Wendy Bussen, and Shaun P Scott. 2009. "Cancer stem cells - from initiation to elimination , how far have we reached ? (Review)." 1491–1503.
- Al-Mehdi, a B, K Tozawa, a B Fisher, L Shientag, a Lee, and R J Muschel. 2000. "Intravascular origin of metastasis from the proliferation of endothelium-attached tumor cells: a new model for metastasis." *Nature medicine* 6(1): 100–2.
- Alitalo, Kari, Tuomas Tammela, and Tatiana V Petrova. 2005. "Lymphangiogenesis in development and human disease." *Nature* 438(7070): 946–53.
- Amatruda, James F, Jennifer L Shepard, Howard M Stern, and Leonard I Zon. 2002. "Zebrafish as a cancer model system." *Cancer cell* 1(3): 229–31.
- Ambros, Inge M, Peter F Ambros, and Sabine Strehl. 1886. "Is a Specific Marker for Ewing's Sarcoma and Peripheral Primitive Neuroectodermal Tumors." 1886–1893.
- Amsterdam A, Sadler KC, Lai K, Farrington S, Bronson RT, Lees JA et al. 2004. "Many ribosomal protein genes are cancer genes in zebrafish". *PLoS Biol* 2: E139
- Andrade, W, Seabrook, T.J, Johnston, M.G, J.B Hay. 1996. "The use of the lipophilic fluorochrome CM-DiI for tracking the migration of lymphocytes. *Journal of Immunological Methods* 194(2): 181- 189.
- André, Nicolas, Arnauld Verschuur, Jochen Rossler, and Jaroslav Sterba. 2010. "Anti-angiogenic therapies for children with cancer." *Current cancer drug targets* 10(8): 879–89.
- Azuma, M, Embree, L.J, Sabaawy H, DD Hickstein. 2007. "Ewing sarcoma protein ewsr1 maintains mitotic integrity and proneural cell survival in the zebrafish embryo." *PLoS ONE* 2:e979
- Bader, A.G., and Vogt, P.K. 2005. "Inhibition of protein synthesis by Y box- binding protein 1 blocks oncogenic cell transformation." *Mol. Cell. Biol.* 25, 2095–2106.
- Bader, Andreas G, Katherine a Felts, Ning Jiang, Hwai Wen Chang, and Peter K Vogt. 2003. "Y box-binding protein 1 induces resistance to oncogenic transformation by the phosphatidylinositol 3-kinase pathway." *Proceedings of the National Academy of Sciences of the United States of America* 100(21): 12384–9.

- Bai, L., & Zhu, W. 2006. "p53 : Structure , Function and Therapeutic Applications. " *Journal of Cancer Molecules* 2(4):141–153.
- Balamuth, Naomi J, and Richard B Womer. 2010. "Ewing ' s sarcoma." *Lancet Oncology* 11(2): 184–192. [http://dx.doi.org/10.1016/S1470-2045\(09\)70286-4](http://dx.doi.org/10.1016/S1470-2045(09)70286-4).
- Basaki, Yuji, Ken-Ichi Taguchi, Hiroto Izumi, Yuichi Murakami, Takuya Kubo, Fumihito Hosoi, Kosuke Watari, Kenji Nakano, Hidetoshi Kawaguchi, Shinji Ohno, Kimitoshi Kohno, Mayumi Ono, and Michihiko Kuwano. 2010. "Y-box binding protein-1 (YB-1) promotes cell cycle progression through CDC6-dependent pathway in human cancer cells." *European journal of cancer (Oxford, England : 1990)* 46(5): 954–65.
- Becker, P.M, Verin, A.D, Booth, A, Liu, F, Birukova, A, J, Garcia. 2001. " Different reguation of diverse physiological responses to VEGF in pulmonary endothelial cells." *American Journal of Physiology* 281: 500– 511.
- Beckman, Mary. 2007. "Zebrafish take the stage in cancer research." *Journal of the National Cancer Institute* 99(7): 500–1.
- Beckwith LG, Moore JL, Tsao-Wu GS, Harshbarger JC, Cheng KC. 2000. "EthylNitrosourea induces neoplasia in zebrafish (Danio rerio)". *Lab Invest* 80: 379–385.
- Berghmans, Stephane, Cicely Jette, David Langenau, Karl Hsu, Rodney Stewart, Thomas Look, and John P Kanki. 2005a. "Making waves in cancer research: new models in the zebrafish." *BioTechniques* 39(2): 227–37.
- Berghmans S, Murphey RD, Wienholds E, Neuberger D, Kutok JL, Fletcher CD et al. 2005b. tp53 mutant zebrafish develop malignant peripheral nerve sheath tumors. *Proc Natl Acad Sci USA* 102: 407–412.
- Bergmann, S, Royer-Pokora, B, Fietze, E, Jürchott, K, Hildebrandt, B, Trost, D, Leenders, F, Claude, J.C, Theuring, F, Bargou, R, Dietel, M, and HD Royer. 2005. "YB-1 provokes breast cancer through the induction of chromosomal instability that emerges from mitotic failure and centrosome amplification." *Cancer research* 65(10): 4078–87.
- Berman, Jason, Karl Hsu, and a Thomas Look. 2003. "Zebrafish as a model organism for blood diseases." *British journal of haematology* 123(4): 568–76.
- Bernstein, Mark, Heinrich Kovar, Michael Paulussen, R Lor Randall, Andreas Schuck, and Lisa A Teot. 2006. "P ediatric O ncolgy Ewing ' s Sarcoma Family of Tumors : Current Management." (C): 503–519.
- Bolontrade, Marcela F, Rong-rong Zhou, and Eugenie S Kleinerman. 2002. "Vasculogenesis Plays a Role in the Growth of Ewing ' s Sarcoma in Vivo Vasculogenesis Plays a Role in the Growth of Ewing ' s Sarcoma." 3622–3627.

- Brabletz, T., Jung, A., Spaderna, S., Hlubek, F., and Kirchner, T. 2005. "Opinion: migrating cancer stem cells - an integrated concept of malignant tumour progression". *Nature Reviews Cancer* 5: 744–749.
- Brown, L.A., Rodaway, A.R., Schilling, T.F., Jowett, T., Ingham, P.W., Patient, R.K., and Sharrocks, A.D. 2000. "Insights into early vasculo- genesis revealed by expression of the ETS-domain transcription factor Fli-1 in wild-type and mutant zebrafish embryos." *Mech. Dev.* 90, 237–252.
- Brown, J Martin, and William R Wilson. 2004. "Exploiting tumour hypoxia in cancer treatment." *Nature reviews. Cancer* 4(6): 437–47.
- Cariati, M, Marlow, R and G. Dontu. 2011. "Cancer Cell Culture" ed. Ian A. Cree. 731(3).
- Carvalho, L, and CP Heisenberg, 2009. "Imaging zebrafish embryos by two-photon excitation time-lapse microscopy." *Methods in molecular biology (Clifton, N.J.)* 546: 273-87
- Chaffer, Christine L, and Robert a Weinberg. 2011. "A perspective on cancer cell metastasis." *Science (New York, N.Y.)* 331(6024): 1559–64.
- Chansky, H.A, Hu, M, Hickstein, D.D, L Yang. 2001. "Oncogenic TLS/ERG and EWS/FLi-1 fusion proteins inhibit RNA splicing mediated by YB-1 protein." *Cancer Research* 61: 3586–3590.
- Chen, Eleanor Y, and David M Langenau. 2011. 105 *Methods in cell biology* 383–402 *Zebrafish models of rhabdomyosarcoma*. Third ed. Elsevier Inc.
- Cheng, Sunfa, Maria Alexandra Alfonso-jaume, Peter R Mertens, and David H Lovett. 2002. "Tumour metastasis suppressor, nm23-beta, inhibits gelatinase A transcription by interference with transactivator Y-box protein-1 (YB-1)." 816: 807–816.
- Cheon, DJ, and S. Orsulic. 2011. "Mouse models of cancer." *Annual Review Pathology* 6:95-119.
- Chi, Jen-Tsan, Z Wang, Di Nuyten, E H Rodriguez, ME Schaner, A Salim, Y Wang, G Kristensen, A Helland, A-L Børresen-Dale, A Giaccia, MT Longaker, T Hastie, GP Yang, M van de Vijver, and P O Brown. 2006. "Gene expression programs in response to hypoxia: cell type specificity and prognostic significance in human cancers." *PLoS medicine* 3(3): e47.
- Cho, R.W., and Clarke, M.F. 2008. "Recent advances in cancer stem cells". *Current. Opinion. Genetic Development.* 18: 1–6.

- Corkery, Dale P, Graham Dellaire, and Jason N Berman. 2011. "Leukaemia xenotransplantation in zebrafish--chemotherapy response assay in vivo." *British journal of haematology* 153(6): 786–9.
- Crane, C.H, Ellis, J, I. Abbruzzese et al. 2006. "Phase I trial evaluating the safety of bevacizumab with concurrent radiotherapy and capecitabine in locally advanced pancreatic cancer." *Journal of Clinical Oncology* 24(7): 1145-1151
- Crawford J, Dale D, G Lyman 2003. "Chemotherapy-induced neutropenia." *Cancer* 100(2): 228–237.
- Criscuoli, Michele L, Mai Nguyen, and Brian P Eliceiri. 2005. "Tumor metastasis but not tumor growth is dependent on Src-mediated vascular permeability." *Blood* 105(4): 1508–14.
- Croce, C.M. 2008. "Oncogenes and cancer." *New England Journal of Medicine* 385(5): 502–512
- Cunnick, G. H., Jiang, W. G., Douglas-Jones, T., Watkins, G., Gomez, K. F., Morgan, M. J., Subramanian, A., et al. 2008. "Lymphangiogenesis and lymph node metastasis in breast cancer." *Molecular Cancer*, 7,:23.
- Da'as S, Teh EM, Dobson JT, Nasrallah GK, McBride ER, Wang H, Neuberg DS, Marshall JS, Lin TJ, Berman JN. 2010. "Zebrafish mast cells demonstrate conserved innate and adaptive immune responses". *Dev. Comp. Immunol.*35:1, 125-34.
- Dalgleish, a G. 2005. "Cancer and Inflammation." *British Journal of Cancer* 92(4): 792–793.
- DeNardo,D.G., Johansson, M, LM. Coussens. 2008. "Immune cells as mediators of solid tumor metastasis." *Cancer Metastasis Review* 27(1): 11-18.
- Detrich, H.W. III, Westerfield, M, Zon, L.I. 1999. "The Zebrafish: Biology." Sandiego: *Methods Cell Biol.* 59:391.
- Le Deley, Marie-Cecile, Olivier Delattre, Karl-Ludwig Schaefer, Sue a Burchill, Gabriele Koehler, Pancras C W Hogendoorn, Thomas Lion, Christopher Poremba, Julien Marandet, Stelly Ballet, Gaelle Pierron, Samantha C Brownhill, Michaela Nesslböck, Andreas Ranft, Uta Dirksen, Odile Oberlin, Ian J Lewis, Alan W Craft, Heribert Jürgens, and Heinrich Kovar. 2010. "Impact of EWS-ETS fusion type on disease progression in Ewing's sarcoma/peripheral primitive neuroectodermal tumor: prospective results from the cooperative Euro-E.W.I.N.G. 99 trial." *Journal of clinical oncology : official journal of the American Society of Clinical Oncology* 28(12): 1982–8.

- van Doorninck, John a, Lingyun Ji, Betty Schaub, Hiroyuki Shimada, Michele R Wing, Mark D Krailo, Stephen L Lessnick, Neyssa Marina, Timothy J Triche, Richard Sposto, Richard B Womer, and Elizabeth R Lawlor. 2010. "Current treatment protocols have eliminated the prognostic advantage of type 1 fusions in Ewing sarcoma: a report from the Children's Oncology Group." *Journal of clinical oncology : official journal of the American Society of Clinical Oncology* 28(12): 1989–94.
- Dobson JT, Seibert J, Teh EM, Da'as SI, Fraser RB, Paw BH, Lin TJ & Berman JN. 2008. "Carboxypeptidase A5 identifies a novel mast cell lineage in the zebrafish providing new insight into mast cell fate determination." *Blood*, 112 (7), 2969-2972.
- Dovey, Michael C, and Leonard I Zon. 2009. "Cancer Stem Cells" ed. John S. Yu. 568: 1–5.
- Eliseeva, I a, E R Kim, S G Guryanov, L P Ovchinnikov, and D N Lyabin. 2011. "Y-box-binding protein 1 (YB-1) and its functions." *Biochemistry. Biokhimiia* 76(13): 1402–33.
- Ellett, Felix, Luke Pase, John W Hayman, Alex Andrianopoulos, and Graham J Lieschke. 2011. "Mpeg1 Promoter Transgenes Direct Macrophage-Lineage Expression in Zebrafish." *Blood* 117(4): e49–56.
- Erb, H E R, Non-small Cell, and Lung Cancer. 2009. "Nuclear Y-Box Binding Protein-1 , a Predictive Marker of Prognosis , Is Correlated with Expression of HER2 / ErbB2." 4(9): 1066–1074.
- Etchin, Julia, John P Kanki, and a Thomas Look. 2011. 105 *Methods in cell biology* 309–37 *Zebrafish as a model for the study of human cancer*. Third ed. Elsevier Inc.
- Evdokimova, Valentina, and Poul H B Sorensen. 2006. "Y-Box Binding Protein 1 Providing a New Angle on Translational Regulation." (June): 1143–1147.
- Evdokimova, Valentina, Cristina Tognon, Tony Ng, Peter Ruzanov, Natalya Melnyk, Dieter Fink, Alexey Sorokin, Lev P Ovchinnikov, Elai Davicioni, Timothy J Triche, and Poul H B Sorensen. 2009. "Translational activation of snail1 and other developmentally regulated transcription factors by YB-1 promotes an epithelial-mesenchymal transition." *Cancer cell* 15(5): 402–15.
- Evdokimova, Valentina, Cristina Tognon, Tony Ng, and Poul H B Sorensen. 2009. "Reduced proliferation and enhanced migration: Two sides of the same coin?" 2901–2906.
- Feitsma, Harma, and Edwin Cuppen. 2008. "Zebrafish as a cancer model." *Molecular cancer research : MCR* 6(5): 685–94.

- Feng, Yi, Cristina Santoriello, Marina Mione, Adam Hurlstone, and Paul Martin. 2010. "Live imaging of innate immune cell sensing of transformed cells in zebrafish larvae: parallels between tumor initiation and wound inflammation." *PLoS biology* 8(12): e1000562.
- Fleischer, R.T, Vollenhoven, B.J, G.C. Weston. 2011. "The effects of chemotherapy and radiotherapy on fertility in premenopausal women." *CME Review Article*. 66(4)248–254.
- Flores, Maria Vega, Christopher J Hall, Kathryn E Crosier, and Philip S Crosier. 2010. "Visualization of embryonic lymphangiogenesis advances the use of the zebrafish model for research in cancer and lymphatic pathologies." *Developmental dynamics : an official publication of the American Association of Anatomists* 239(7): 2128–35.
- Folkman, Judah. 2006. "Angiogenesis." *Annual review of medicine* 57: 1–18.
- Forrester, AM, Grabher,C, McBridde, ER, Boyd, ER, Vigerstad, MH, Edgar, A, Kai, FB, Da'as, SI, Payne,E, Look, AT, Berman, JN. 2011. "NUP98-HOXA9-transgenic zebrafish develop a myeloproliferative neoplasm and provide new insight into mechanisms of myeloid leukaemogenesis." *British Journal of Haematology*. 155(2): 167–181.
- Fujita, Jun. 1999. "Cold shock response in mammalian cells." *Journal of molecular microbiology and biotechnology*. 1(2): 243-255.
- Gerber, Hans-peter, Joe Kowalski, Daniel Sherman, Hans-peter Gerber, Joe Kowalski, Daniel Sherman, David A Eberhard, and Napoleone Ferrara. 2000. "Complete Inhibition of Rhabdomyosarcoma Xenograft Growth and Neovascularization Requires Blockade of Both Tumor and Host Vascular Endothelial Growth Factor Advances in Brief Complete Inhibition of Rhabdomyosarcoma Xenograft Growth and Neovascularization Requires Blockade of Both Tumor and Host Vascular Endothelial Growth Factor." 6253–6258.
- Giatromanolaki, Alexandra, Maria Bai, Dimitrios Margaritis, Konstantinos L Bourantas, Michael I Koukourakis, Efthimios Sivridis, and Kevin C Gatter. 2010. "Hypoxia and activated VEGF/receptor pathway in multiple myeloma." *Anticancer research* 30(7): 2831–6.
- Ginsberg, B. J. P., Alava, E. D., Ladanyi, M., Wexler, L. H., Kovar, H., Paulussen, M., Zoubek, A., et al. 1999. "EWS-FLII and EWS-ERG gene fusions are associated with similar clinical phenotypes in Ewing's sarcoma." 17(6), 1809–1814.
- Gluz, Oleg, Karin Mengele, Manfred Schmitt, Ronald Kates, Raihana Diallo-Danebrock, Frauke Neff, Hans-Dieter Royer, Niels Eckstein, Svjetlana Mohrmann, Evelyn Ting, Marion Kiechle, Christopher Poremba, Ulrike Nitz, and Nadia Harbeck. 2009. "Y-box-

- binding protein YB-1 identifies high-risk patients with primary breast cancer benefiting from rapidly cycled tandem high-dose adjuvant chemotherapy.” *Journal of clinical oncology : official journal of the American Society of Clinical Oncology* 27(36): 6144–51.
- Granowetter, Linda, Richard Womer, Meenakshi Devidas, Mark Krailo, Chenguang Wang, Mark Bernstein, Neyssa Marina, Patrick Leavey, Mark Gebhardt, John Healey, Robert Cooper Shamberger, Allen Goorin, James Miser, James Meyer, Carola a S Arndt, Scott Sailer, Karen Marcus, Elizabeth Perlman, Paul Dickman, and Holcombe E Grier. 2009. “Dose-intensified compared with standard chemotherapy for nonmetastatic Ewing sarcoma family of tumors: a Children’s Oncology Group Study.” *Journal of clinical oncology : official journal of the American Society of Clinical Oncology* 27(15): 2536–41.
- Gupta, G.P, and J. Massague. 2006. "Cancer Metastasis: building a framework." *Cell Review* 127: 679–695.
- Haldi, Maryann, Christopher Ton, Wen Lin Seng, and Patricia McGrath. 2006. “Human melanoma cells transplanted into zebrafish proliferate, migrate, produce melanin, form masses and stimulate angiogenesis in zebrafish.” *Angiogenesis* 9(3): 139–51.
- Hanahan, D, and J Folkman. 1996. “Patterns and emerging mechanisms of the angiogenic switch during tumorigenesis.” *Cell* 86(3): 353–64.
- Hanahan, D, R A Weinberg. 2000. “The Hallmarks of Cancer.” *Cell Press* 100: 57–70.
- Hanahan, D, R A Weinberg. 2011. “The Hallmarks of Cancer: The Next Generation" *Cell Review* 144: 646–674.
- Hart, A., Melet, F., Grossfeld, P., Chien, K., Jones, C., Tunnacliffe, A., Favier, R., et al. 2000. "Fli-1 Is required for murine vascular and megakaryocytic development and is hemizygotously deleted in patients with thrombocytopenia." *Canadian Institutes of Health Research*, 13, 167–177.
- Hartenstein, Bettina, Bernd Thilo Dittrich, Dominique Stickens, Babette Heyer, Thiennu H Vu, Sibylle Teurich, Marina Schorpp-Kistner, Zena Werb, and Peter Angel. 2006. “Epidermal development and wound healing in matrix metalloproteinase 13-deficient mice.” *The Journal of investigative dermatology* 126(2): 486–96.
- He, Shuning, Gerda Em Lamers, Jan-Willem M Beenakker, Chao Cui, Veerander Ps Ghotra, Erik Hj Danen, Annemarie H Meijer, Herman P Spaink, and B Ewa Snaar-Jagalska. 2012. “Neutrophil-mediated experimental metastasis is enhanced by VEGFR inhibition in a zebrafish xenograft model.” *The Journal of pathology* 227(4): 431–45.
- Heare, Travis, Mary a Hensley, and Shelley Dell’Orfano. 2009. “Bone tumors: osteosarcoma and Ewing’s sarcoma.” *Current opinion in pediatrics* 21(3): 365–72.

- Hedley, Benjamin D, and Ann F Chambers. 2009. "Tumor dormancy and metastasis." *Advances in cancer research* 102(09): 67–101.
- Heine, a, S a E Held, a Bringmann, T a W Holderried, and P Brossart. 2011. "Immunomodulatory effects of anti-angiogenic drugs." *Leukemia : official journal of the Leukemia Society of America, Leukemia Research Fund, U.K* 25(6): 899–905.
- Hense, H W, S Ahrens, M Paulussen, M Lehnert, and H Jiirgens. 1999. "Original article Factors associated with tumor volume and primary metastases in Ewing tumors : Results from the (EI) CESS studies." 1073–1077.
- Johnson, J R, W G Hammond, J R Benfield, and H Tesluk. 1995. "Successful xenotransplantation of human lung cancer correlates with the metastatic phenotype." *The Annals of thoracic surgery* 60(1): 32–6; discussion 36–7.
- Kaya, M, T Wada, S Nagoya, M Sasaki, T Matsumura, and T Yamashita. 2009. "The level of vascular endothelial growth factor as a predictor of a poor prognosis in osteosarcoma." *The Journal of bone and joint surgery. British volume* 91(6): 784–8.
- Kees, Tim, and Mikala Egeblad. 2011. "Innate immune cells in breast cancer--from villains to heroes?" *Journal of mammary gland biology and neoplasia* 16(3): 189–203.
- Khanna, Chand, Xiaolin Wan, Seuli Bose, Ryan Cassaday, Osarenoma Olomu, Arnulfo Mendoza, Choh Yeung, Richard Gorlick, Stephen M Hewitt, and Lee J Helman. 2004. "The membrane-cytoskeleton linker ezrin is necessary for osteosarcoma metastasis." *Nature medicine* 10(2): 182–6.
- Kilic, M, H Kasperczyk, S Fulda, and K-M Debatin. 2007. "Role of hypoxia inducible factor-1 alpha in modulation of apoptosis resistance." *Oncogene* 26(14): 2027–38.
- Kohno, Kimitoshi, Hiroto Izumi, Takeshi Uchiumi, Megumi Ashizuka, and Michihiko Kuwano. 2003. "The pleiotropic functions of the Y-box-binding protein, YB-1." *BioEssays : news and reviews in molecular, cellular and developmental biology* 25(7): 691–8.
- Kumar, Ramakant, Sukesh Sankineani, Shishir Rastogi, Shyam Prakash, Sameer Bakhshi, Mehar C Sharma, Shahalam Khan, Gopal Sagar Dc, and Laxman Rijal. 2012. "Expression of Vascular endothelial growth factor in Ewing's sarcoma." *International orthopaedics* 36(8): 1669–72.
- Kuttesch, By John F, Leonard H Wexler, Robert B Marcus, Diane Fairclough, Linda Weaver-mcclure, Margaret White, Lion Mao, Thomas F Delaney, Charles B Pratt, Marc E Horowitz, and Larry E Kun. 2012. "Second Malignancies After Ewing ' s Sarcoma : Radiation Dose-Dependency of Secondary Sarcomas." 14(10): 2818–2825.

- Kuttesch, J F. 1996. "Multidrug resistance in pediatric oncology." *Investigational new drugs* 14(1): 55–67.
- Lam, S.H, H.L Chua, Z Gong, T.J Lam, and Y.M Sin. 2004. "Development and maturation of the immune system in zebrafish, *Danio rerio*: a gene expression profiling, in situ hybridization and immunological study." *Developmental & Comparative Immunology* 28(1): 9–28.
- Lam SH, Gong Z. 2006. "Modeling liver cancer using zebrafish: a comparative oncogenomics approach". *Cell Cycle* 5: 573–577.
- Langenau, David M, Matthew D Keefe, Narie Y Storer, Jeffrey R Guyon, Jeffery L Kutok, Xiuning Le, Wolfram Goessling, Donna S Neuberg, Louis M Kunkel, and Leonard I Zon. 2007. "Effects of RAS on the genesis of embryonal rhabdomyosarcoma." *Genes & development* 21(11): 1382–95.
- Langenau, David M, David Traver, Adolfo a Ferrando, Jeffery L Kutok, Jon C Aster, John P Kanki, Shuo Lin, Ed Prochownik, Nikolaus S Trede, Leonard I Zon, and a Thomas Look. 2003. "Myc-induced T cell leukemia in transgenic zebrafish." *Science (New York, N.Y.)* 299(5608): 887–90.
- Lawson, Nathan D., and Brant M. Weinstein. 2002. "In Vivo Imaging of Embryonic Vascular Development Using Transgenic Zebrafish." *Developmental Biology* 248(2): 307–318.
- Le, Xiuning, David M Langenau, Matthew D Keefe, Jeffery L Kutok, Donna S Neuberg, and Leonard I Zon. 2007. "Heat shock-inducible Cre/Lox approaches to induce diverse types of tumors and hyperplasia in transgenic zebrafish." *Proceedings of the National Academy of Sciences of the United States of America* 104(22): 9410–5.
- Leacock, Stefanie W, Audrey N Basse, Garvin L Chandler, Anne M Kirk, Dinesh Rakheja, and James F Amatruda. 2012. "A zebrafish transgenic model of Ewing's sarcoma reveals conserved mediators of EWS-FLI1 tumorigenesis." *Disease models & mechanisms* 5(1): 95–106.
- Lee, Lisa M J, Elisabeth a Seftor, Gregory Bonde, Robert a Cornell, and Mary J C Hendrix. 2005. "The fate of human malignant melanoma cells transplanted into zebrafish embryos: assessment of migration and cell division in the absence of tumor formation." *Developmental dynamics : an official publication of the American Association of Anatomists* 233(4): 1560–70.
- Liu, S, S.D Leach. 2011. "Zebrafish models for cancer." *The Annual Review of Pathology* 6: 71-93

- Lu, Jeng-Wei, Yu Hsia, Hsiao-Chen Tu, Yung-Chun Hsiao, Wan-Yu Yang, Horng-Dar Wang, and Chiou-Hwa Yuh. 2011. "Liver development and cancer formation in zebrafish." *Birth defects research. Part C, Embryo today : reviews* 93(2): 157–72.
- Ludwig, Joseph a. 2008. "Ewing sarcoma: historical perspectives, current state-of-the-art, and opportunities for targeted therapy in the future." *Current opinion in oncology* 20(4): 412–8.
- Mandrekar, Noopur, and Narsinh L Thakur. 2009. "Significance of the zebrafish model in the discovery of bioactive molecules from nature." *Biotechnology letters* 31(2): 171–9.
- Marques, Ines J, Frank Ulrich Weiss, Danielle H Vlecken, Claudia Nitsche, Jeroen Bakkers, Anne K Lagendijk, Lars Ivo Partecke, Claus-Dieter Heidecke, Markus M Lerch, and Christoph P Bagowski. 2009. "Metastatic behaviour of primary human tumours in a zebrafish xenotransplantation model." *BMC cancer* 9: 128.
- Martina, K, Balci TB, Hartwig, UF, Dellaire, G, Andre, MC, Berman, JN, C. Lengerke. 2012. Zebrafish xenografts as a tool for in vivo studies on human cancer." *Animals of the New York Academy of Sciences*
- Matsumoto, Ken, and Boon-Huat Bay. 2005. "Significance of the Y-box proteins in human cancers." *Journal of molecular and genetic medicine : an international journal of biomedical research* 1(1): 11–7.
- McCawley, L J, and L M Matrisian. 2000. "Matrix metalloproteinases: multifunctional contributors to tumor progression." *Molecular medicine today* 6(4): 149–56.
- Mehlen, Patrick, and Alain Puisieux. 2006. "Metastasis: a question of life or death." *Nature reviews. Cancer* 6(6): 449–58.
- Merk, LP, Adams, RA, Poole Merk, L and RA Adams. 1972. "Effects of Infant Thymectomy and Antilymphocyte Serum on Xenotransplantation of a Human Leukemia in the Hamster Effects of Infant Thymectomy and Antilymphocyte Serum on Xenotransplantation of a Human Leukemia in the Hamster1." 1580–1583.
- Mizgireuv IV, Majorova IG, Gorodinskaya VM, Khudoley VV, SY Revskoy . 2004. "Carcinogenic effect of N-nitrosodimethylamine on diploid and triploid zebrafish (Danio rerio)". *Toxicology Pathology* 5: 514–518.
- Monsuez, J.-J., Charniot, J.-C., Vignat, N., & Artigou, J.-Y. 2010. "Cardiac side-effects of cancer chemotherapy." *International journal of cardiology*, 144(1), 3–15.
- Mouneimne, Ghassan, and Joan S Brugge. 2009. "YB-1 translational control of epithelial-mesenchyme transition." *Cancer cell* 15(5): 357–9.

- Muschel, Ruth J, and Annamaria Gal. 2008. "Tetraspanin in oncogenic epithelial-mesenchymal transition." 118(4): 1347–1350.
- Nash, G F, L F Turner, M F Scully, and A K Kakkar. 2002. "Review." 3(July): 425–430.
- Nguyen, Don X, Paula D Bos, and Joan Massagué. 2009. "Metastasis: from dissemination to organ-specific colonization." *Nature reviews. Cancer* 9(4): 274–84.
- Nicoli, Stefania, and Marco Presta. 2007. "The zebrafish/tumor xenograft angiogenesis assay." *Nature protocols* 2(11): 2918–23.
- Oda, Y, Sakamoto, A, Shinohara, N, Ohga, T, Uchiumi, T, Kohno, K, Tsuneyoshi, M, Kuwano, M, Y. Iwamoto. 1998. "Nuclear expression of YB-1 protein correlates with P-glycoprotein expression in human osteosarcoma." *Clinical Cancer Research*. 4(9): 2273-2277.
- Oda, Yoshinao, Yoshihiro Ohishi, Tsuyoshi Saito, Eiji Hinoshita, Takeshi Uchiumi, Naoko Kinukawa, Yukihide Iwamoto, Kimitoshi Kohno, Michihiko Kuwano, and Masazumi Tsuneyoshi. 2003. "Nuclear expression of Y-box-binding protein-1 correlates with P-glycoprotein and topoisomerase II alpha expression, and with poor prognosis in synovial sarcoma." *The Journal of pathology* 199(2): 251–8.
- Okamoto, T, H Izumi, T Imamura, H Takano, T Ise, T Uchiumi, M Kuwano, and K Kohno. 2000. "Direct interaction of p53 with the Y-box binding protein, YB-1: a mechanism for regulation of human gene expression." *Oncogene* 19(54): 6194–202.
- Okihiro MS, DE Hinton. 1999. Progression of hepatic neoplasia in medaka (*Oryzias latipes*) exposed to diethylnitrosamine. *Carcino- genesis* 20: 933–940.
- Ordóñez, José Luis, Daniel Osuna, David Herrero, Enrique de Alava, and Juan Madoz-Gúrpide. 2009. "Advances in Ewing's sarcoma research: where are we now and what lies ahead?" *Cancer research* 69(18): 7140–50.
- Overall, C M, and O Kleifeld. 2006. "Towards third generation matrix metalloproteinase inhibitors for cancer therapy." *British journal of cancer* 94(7): 941–6.
- Patton, Zon, L. 2005. "Taking Human Cancer Genes to the Fish : MELANOMA : A LETHAL CANCER." 1(4): 363–368.
- Paulussen, M, Bielack, S, Jurgens, H, Casali, PG: ESMO Guidelines Working Group. 2009. "Ewing's sarcoma of the bone: EMSO clinical recommendations for diagnosis, treatment and follow-up." *Annual Onocology* 4: 140-142.
- Payne, Elspeth, and Thomas Look. 2009. "Zebrafish modelling of leukaemias." *British journal of haematology* 146(3): 247–56.

- Peltier, Leonard. 1984. "Diffuse endothelioma of bone. By James Ewing, 1921.pdf." *The Classic* (185): 2–5.
- Plougastel, B, J Zucman, M Peter, G Thomas, and O Delattre. 1993. "Genomic structure of the EWS gene and its relationship to EWSR1, a site of tumor-associated chromosome translocation." *Genomics* 18(3): 609–15.
- Puchalski, a. 2010. "Ewing Sarcoma Family of Tumors." *Journal of Diagnostic Medical Sonography* 26(5): 238–244.
- Quan, Gerald M Y, and Peter F M Choong. 2006. "Anti-angiogenic therapy for osteosarcoma." *Cancer metastasis reviews* 25(4): 707–13.
- Quesada, Ana R, Ramón Muñoz-Chápuli, and Miguel a Medina. 2006. "Anti-angiogenic drugs: from bench to clinical trials." *Medicinal research reviews* 26(4): 483–530.
- Ravi, R, Mookerjee, B, Bhujwalla Z.M, , Hayes Sutter, C, Artemov, D, Zeng, Q, Dillehay, L, Madan, A, Semenza, G.L, A. Bedi. 2000. "Regulation of tumor angiogenesis by p53-induced degradation of hypoxia-inducible factor 1 α ." *Genes Dev.* 14, 34–44
- Renshaw, Stephen a, Catherine a Loynes, Daniel M I Trushell, Stone Elworthy, Philip W Ingham, and Moira K B Whyte. 2006. "A transgenic zebrafish model of neutrophilic inflammation." *Blood* 108(13): 3976–8.
- Riggi, Nicolo, Mario-Luca Suva, and Ivan Stamenkovic. 2009. "Ewing's sarcoma origin: from duel to duality." *Expert review of anticancer therapy* 9(8): 1025–30.
- Riggi, Nicolò, and Ivan Stamenkovic. 2007. "The Biology of Ewing sarcoma." *Cancer letters* 254(1): 1–10.
- Riggi, Nicolò, Mario-Luca Suvà, Domizio Suvà, Luisa Cironi, Paolo Provero, Stéphane Tercier, Jean-Marc Joseph, Jean-Christophe Stehle, Karine Baumer, Vincent Kindler, and Ivan Stamenkovic. 2008. "EWS-FLI-1 expression triggers a Ewing's sarcoma initiation program in primary human mesenchymal stem cells." *Cancer research* 68(7): 2176–85.
- Rowe, H, and J H Stolar. 2000. "Anti-VEGF Antibody Suppresses and Metastasis in an Experimental." 35(1): 30–33.
- Saji, Hisashi, Masakazu Toi, Shigehira Saji, Morio Koike, Kimitoshi Kohno, and Michihiko Kuwano. 2003. "Nuclear expression of YB-1 protein correlates with P-glycoprotein expression in human breast carcinoma." *Cancer letters* 190(2): 191–7.

- Segerström, Lova, Dieter Fuchs, Ulrika Bäckman, Kajsa Holmquist, Rolf Christofferson, and Faranak Azarbayjani. 2006. "The anti-VEGF antibody bevacizumab potently reduces the growth rate of high-risk neuroblastoma xenografts." *Pediatric research* 60(5): 576–81.
- Semenza, Gregg L. 2003. "Targeting HIF-1 for cancer therapy." *Nature reviews. Cancer* 3(10): 721–32.
- Serbedzija, George N, Edward Flynn, and Catherine E Willett. 2000. "Zebra ® sh angiogenesis : A new model for drug screening." (ICM).
- Shepard JL, Amatruda JF, Stern HM, Subramanian A, Finkelstein D, Ziai J et al. 2005. "A zebrafish bmyb mutation causes genome instability and increased cancer susceptibility." *Proc Natl* 102: 13194–13199.
- Shing, Danielle C, Dominic J McMullan, Paul Roberts, Danielle C Shing, Dominic J McMullan, Paul Roberts, Kim Smith, Suet-feung Chin, James Nicholson, Roger M Tillman, Pramila Ramani, Catherine Cullinane, and Nicholas Coleman. 2003. "FUS / ERG Gene Fusions in Ewing ' s Tumors FUS / ERG Gene Fusions in Ewing ' s Tumors." 4568–4576.
- Simmons Kovacs, L. A. S., Orlando, D. A., & S. B. Haase 2008. Transcription networks and cyclin/CDKs." *Cell Cycle* 7(17):2626–2629.
- Smith, T. G., Robbins, P. a, & P.J Ratcliffe, P. J. 2008. "The human side of hypoxia-inducible factor." *British journal of haematology*, 141(3):325–34
- Spano, D., Heck, C., De Antonellis, P., Christofori, G., & Zollo, M. 2012. "Molecular networks that regulate cancer metastasis". *Seminars in cancer biology*, 22(3), 234–49.
- Stoletov, K, and R Klemke. 2008. "Catch of the day: zebrafish as a human cancer model." *Oncogene* 27(33): 4509–20.
- Streisinger, G, Walker, C, Dower, N, Knauber, D, F. 1981. "Production of clones of homozygous diploid zebrafish (Brachydanio rerio)." *Nature* 291: 293-296.
- Szuhai, K, IJszenga, M, Tanke, H.J, Rosenberg, C, P Hogendoorn. 2005. "Molecular cytogenetic characterization of four previously established and two newly established Ewing sarcoma cell lines." *Cancer Genetics and Cytogenetics* 166: 173-179.
- Taylor, A.M, and L.I Zon. 2009. "Zebrafish tumor assays: the state of transplantation." *Zebrafish* 6(4): 339–346.

- Thiery, Jean Paul. 2002. "Epithelial-mesenchymal transitions in tumour progression." *Nature reviews. Cancer* 2(6): 442–54.
- Tirode, Franck, Karine Laud-Duval, Alexandre Prieur, Bruno Delorme, Pierre Charbord, and Olivier Delattre. 2007. "Mesenchymal stem cell features of Ewing tumors." *Cancer cell* 11(5): 421–9.
- Traver, David, Philippe Herbomel, E Elizabeth Patton, Ryan D Murphey, Jeffrey a Yoder, Gary W Litman, André Catic, Chris T Amemiya, Leonard I Zon, and Nikolaus S Trede. 2003. "The zebrafish as a model organism to study development of the immune system." *Advances in immunology* 81: 253–330.
- Weis, Sara M, and David a Cheresch. 2005. "Pathophysiological consequences of VEGF-induced vascular permeability." *Nature* 437(7058): 497–504.
- White, Richard Mark, Anna Sessa, Christopher Burke, Teresa Bowman, Jocelyn LeBlanc, Craig Ceol, Caitlin Bourque, Michael Dovey, Wolfram Goessling, Caroline Erter Burns, and Leonard I Zon. 2008. "Transparent adult zebrafish as a tool for in vivo transplantation analysis." *Cell stem cell* 2(2): 183–9.
- Whiteside, Theresa L. 2006. "Immune suppression in cancer: effects on immune cells, mechanisms and future therapeutic intervention." *Seminars in cancer biology* 16(1): 3–15.
- Williams, J Lynne. 2012. "Cancer stem cells." *Clinical laboratory science : journal of the American Society for Medical Technology* 25(1): 50–7.
- Windsor, Rachael, Sandra Strauss, Beatrice Seddon, and Jeremy Whelan. 2009. "Experimental therapies in Ewing's sarcoma." *Expert opinion on investigational drugs* 18(2): 143–59.
- Wu, Yadi, Jiong Deng, Piotr G Rychahou, Suimin Qiu, B Mark Evers, and Binhua P Zhou. 2009. "Stabilization of snail by NF-kappaB is required for inflammation-induced cell migration and invasion." *Cancer cell* 15(5): 416–28.
- Wu, Ying, Sohsuke Yamada, Hiroto Izumi, Zhi Li, Shohei Shimajiri, Ke-Yong Wang, Yun-Peng Liu, Kimitoshi Kohno, and Yasuyuki Sasaguri. 2012. "Strong YB-1 expression is associated with liver metastasis progression and predicts shorter disease-free survival in advanced gastric cancer." *Journal of surgical oncology* 105(7): 724–30.
- Wyatt, Rachael a, Jonathan Y Keow, Natalie D Harris, Charles a Haché, Daniel H Li, and Bryan D Crawford. 2009. "The zebrafish embryo: a powerful model system for investigating matrix remodeling." *Zebrafish* 6(4): 347–54.

- Yang, Hong Wei, Jeffery L Kutok, Nam Hyuk Lee, Hui Ying Piao, Christopher D M Fletcher, John P Kanki, and a Thomas Look. 2004. "Targeted expression of human MYCN selectively causes pancreatic neuroendocrine tumors in transgenic zebrafish." *Cancer research* 64(20): 7256–62.
- Yang, J.C, Haworth, R, M. Sherry et al. 2003. "A randomized trial of bevacizumab, an anti-vascular endothelial growth factor antibody, for metastatic renal cancer." *New England Journal of Medicine* 349(5): 427-434
- Yokota, J. 2000. "Tumor progression and metastasis." *Carcinogenesis* 21(3): 497–503.
- Yu, Joanne L, and Janusz W Rak. 2003. "Host microenvironment in breast cancer development Inflammatory and immune cells in tumour angiogenesis and arteriogenesis." 83–88.
- Zetter, B R. 1998. "Angiogenesis and tumor metastasis." *Annual review of medicine* 49(1): 407–24.
- Zhang, P J, M Barcos, C C Stewart, a W Block, S Sait, and J J Brooks. 2000. "Immunoreactivity of MIC2 (CD99) in acute myelogenous leukemia and related diseases." *Modern pathology : an official journal of the United States and Canadian Academy of Pathology, Inc* 13(4): 452–8.
- Zhao, Chengjian, Xiaofei Wang, Yuwei Zhao, Zhimian Li, Shuo Lin, Yuquan Wei, and Hanshuo Yang. 2011. "A novel xenograft model in zebrafish for high-resolution investigating dynamics of neovascularization in tumors." *PloS one* 6(7): e21768.

**Appendix A: Relative Risk Estimates for TC32 ctrl Compared to Fixed TC32
ctrl cells**

Group * Cells In Tail Crosstabulation

		InTail		Total
		No	Yes	
TC32 cells	Count	25.0	67.0	92.0
	Expected Count	53.3	38.7	92.0
Fixed TC32 cells	Count	77.0	7.0	84.0
	Expected Count	48.7	35.3	84.0
Total	Count	102.0	74.0	176.0
	Expected Count	102.0	74.0	176.0

Chi-Square Tests

	Value	df	p- value
Pearson Chi-Square	74.950	1	.000
Likelihood ratio	83.689	1	.000
N of Valid Cases	176.0		

Risk Estimate		95% Confidence Interval	
	Value	Lower	Upper
Odds ratio for Group (ctrl/fixed)	0.034	0.014	0.083
For cohort In Tail = Yes	8.739	4.253	17.957

TC32 ctrl cells are 8.739X more likely to migrate to the tail, compared to fixed TC32 cells

Appendix B: Relative Risk Estimates for TC32 ctrl Compared to TC32 YB-1

kd cells

Group * Cells In Tail Crosstabulation

		InTail		Total
		No	Yes	
TC32 ctrl cells	Count	25.0	67.0	92.0
	Expected Count	48.3	43.7	92.0
TC32 YB-1 kd cells	Count	70.0	19.0	89.0
	Expected Count	46.7	42.3	89.0
Total	Count	95.0	86.0	181.0
	Expected Count	95.0	86.0	181.0

Chi-Square Tests

	Value	df	p- valve
Pearson Chi-Square	48.070	1	.000
Likelihood ratio	50.536	1	.000
N of Valid Cases	181.0		

Risk Estimate	Value	95% Confidence Interval	
		Lower	Upper
Odds ratio for Group (ctrl/kd)	0.101	0.051	0.201
For cohort In Tail = Yes	3.411	2.246	5.181

TC32 ctrl cells are 3.411X more likely to migrate to the tail, compared to to TC32 YB-1 kd cells

Appendix C: Copyright Permission



The official journal of the Society for Translational Oncology

August 24, 2012

Chansey Veinotte
MSc. Candidate
Berman Zebrafish Lab/ IWK Health Centre
Dalhousie University
Department of Microbiology & Immunology

Dear Mr. Veinotte;

We are pleased to grant you permission to reuse Figure 1 (Primary tumor sites in Ewing's tumors. Data based on 1,426 patients from European Intergroup Cooperative Ewing Sarcoma Studies Trials.) from "Ewing's Sarcoma Family of Tumors: Current Management" by Mark Bernstein, Heinrich Kovar, Michael Paulussen, et al., published in *The Oncologist* 2006; 11:503-519; doi:10.1634/theoncologist.11-5-503.

This figure will be reproduced and included in your master thesis.

The granting of this permission is exclusively limited to the above-stated usage, provided that full credit is given to *The Oncologist* in the respective reference.

Please sign and return this disclaimer.

Disclaimer: Material published in *The Oncologist* is protected by copyright. The granting of permission to adapt the figure is solely limited to this one-time usage, and does not include any other figure or article. In addition to the Disclaimer, *The Oncologist*, AlphaMed Press, publisher of *The Oncologist*, the Editorial Board of the Journal, and the respective employees, officers and agents accept no liability whatsoever for the consequences of any inaccurate or misleading data, opinion or statement.

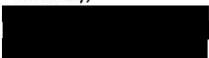
[PRINT NAME] Chansey J Veinotte

SIGNATURE  August 24th 2012

The royalty fee for this request has been waived.

We appreciate your interest in *The Oncologist* and look forward to receiving your signed Disclaimer.

Sincerely,


Ann Murphy, Ph.D.
Managing Editor
THE ONCOLOGIST
318 Blackwell Street, Suite 260
Durham, North Carolina 27701
AnnMurphy@TheOncologist.com